Volume 275, Number 11, November 2014

JOURNAL OF

morphology

ISSN 0362-2525

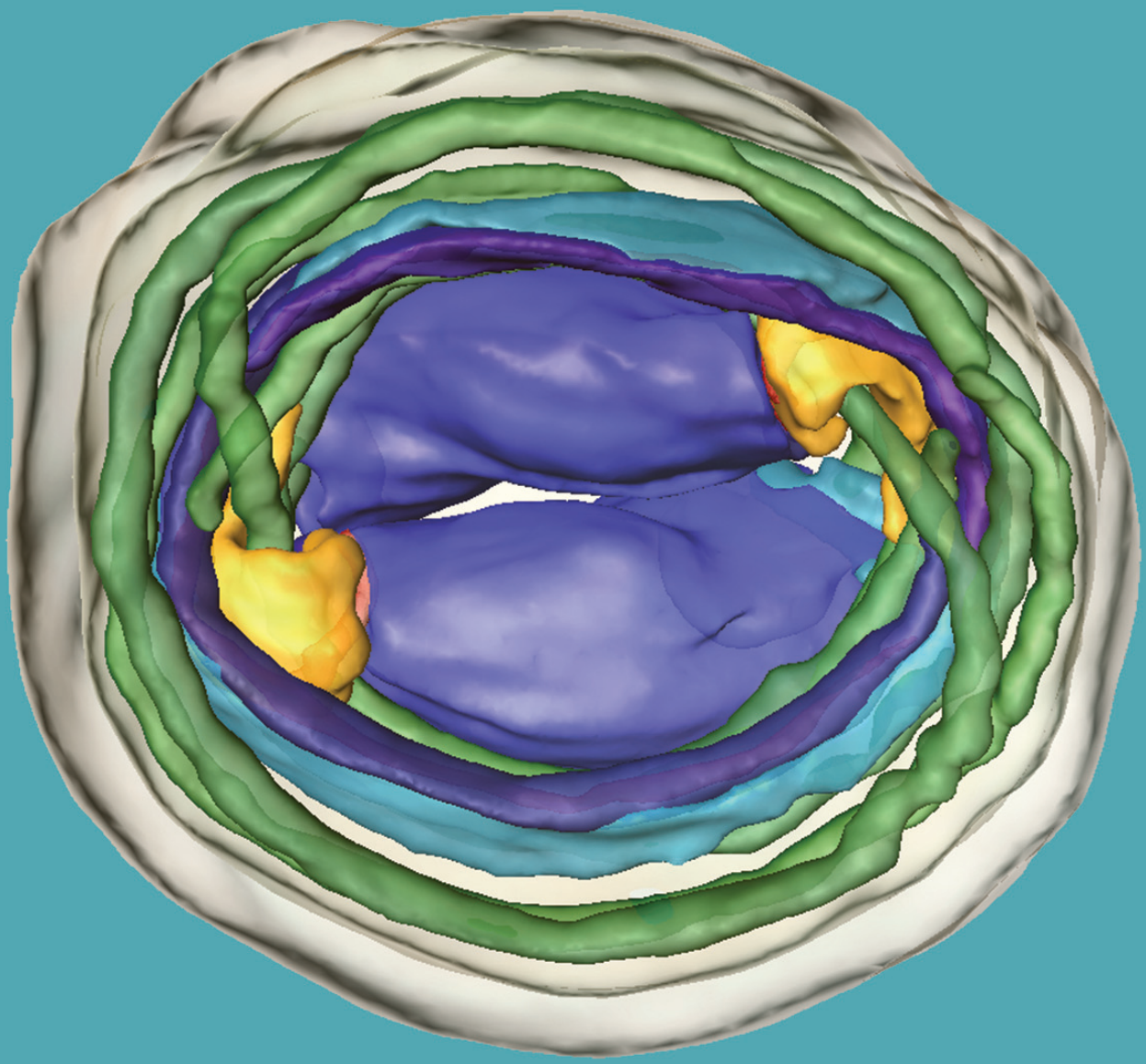

WILEY Blackwell

JOURNAL OF MORPHOLOGY welcomes articles of original research in cytology, protozoology, embryology, general, comparative and functional morphology. Preliminary notices or articles of a purely taxonomic or ecological nature are not included. No paper which has already appeared will be accepted nor will simultaneous publications elsewhere be allowed. Manuscripts may now be submitted online via Manuscript Central at http://mc.manuscriptcentral.com/jmor.

JOURNAL OF MORPHOLOGY, (Print ISSN 0362-2525; Online ISSN 1097-4687), is published monthly by Wiley Subscription Services, Inc., a Wiley Company, 111 River St., Hoboken, NJ 07030-5774. Periodicals postage paid at Hoboken, NJ, and at additional mailing offices. Postmaster: Send all address changes to JOURNAL OF MORPHOLOGY, John Wiley & Sons Inc., C/O The Sheridan Press, PO Box 465, Hanover, PA 17331. **Information for subscribers:** JOURNAL OF MORPHOLOGY is published in 12 issues per year. Institutional subscription prices for 2014 are: Print & Online: US$9,328 (US), US$9,496 (Canada and Mexico), £4,913 (UK), €6,213 (Europe), US$9,580 (Rest of World). Prices are exclusive of tax. Asia-Pacific GST, Canadian GST/HST and European VAT will be applied at the appropriate rates. For more information on current tax rates, please go to www.wileyonlinelibrary.com/tax-vat. The price includes online access to the current and all online back files to January 1st 2010, where available. For other pricing options, including access information and terms and conditions, please visit www.wileyonlinelibrary.com/access. **Back issues:** Single issues from current and recent volumes are available at the current single issue price from cs-iournals@wiley.com. Earlier issues may be obtained from Periodicals Service Company, 11 Main Street, Germantown, NY 12526, USA. Tel: +1 518 537 4700, Fax: +1 518 537 5899, Email: psc@periodicals.com. **Delivery Terms and Legal Title:** Where the subscription price includes print issues and delivery is to the recipient's address, delivery terms are Delivered at Place (DAP); the recipient is responsible for paying any import duty or taxes. Title to all issues transfers FOB our shipping point, freight prepaid. We will endeavour to fulfil claims for missing or damaged copies within six months of publication, within our reasonable discretion and subject to availability. **Journal Customer Services:** For ordering information, claims and any enquiry concerning your journal subscription please go to www.wileyonlinelibrary.com/ask or contact your nearest office. **Americas:** Email: cs-journals@ wiley.com; Tel: +1 781 388 8598 or +1 800 835 6770 (toll free in the USA & Canada). **Europe, Middle East and Africa:** Email: cs-journals@ wiley.com; Tel: +44 (0) 1865 778315. **Asia Pacific:** Email: cs-journals@wiley.com; Tel: +65 6511 8000. **Japan:** For Japanese speaking support, Email: cs-japan@wiley.com; Tel: +65 6511 8010 or Tel (toll-free): 005 316 50 480. **Visit our Online Customer Get-Help** available in 6 languages at www.wileycustomerhelp.com. Claims for undelivered copies will be accepted only after the following issue has been received. Please enclose a copy of the mailing label or cite your subscriber reference number in order to expedite handling. Missing copies will be supplied when losses in transit and where reserve stock permits. If claims are not resolved satisfactorily, please write Journal Customer Services. **Production Editor:** Nick DeAngelis (email: jrnlprodjmor@cadmus.com). **Advertising:** Advertising Sales Manager, 111 River Street, Hoboken, NJ 07030, Tel: +1 201 748-8832; Fax: +1 201 748-6207. **Commercial Reprints:** E-mail: corporatesaleseurope@wiley.com; corporatesalesusa@wiley.com; or corporatesalesaustralia@wiley.com. **Author Reprints (50–500 copies):** Order online: http://www.sheridanreprints.com/orderForm.html. E-mail: chris.jones@sheridan.com. **Note to NIH Grantees:** Pursuant to NIH mandate, Wiley-Blackwell will post the accepted version of contributions authored by NIH grant-holders to PubMed Central upon acceptance. This accepted version will be made publicly available 12 months after publication. For further information, see www.wiley.com/go/nihmandate. For submission instructions, subscription and all other information visit: wileyonlinelibrary.com/journal/jmor. JOURNAL OF MORPHOLOGY accepts articles for Open Access publication. Please visit http://olabout.wiley.com/WileyCDA/Section/id-406241.html for further information about OnlineOpen.

Abstracting and Indexing Services: The Journal is indexed by ASFA: Aquatic Sciences & Fisheries Abstracts; BIOBASE: Current Awareness in Biological Sciences; Biological Abstracts; BIOSIS Previews; CAS: Chemical Abstracts Service; Chemical Abstracts Service/SciFinder; CSA Biological Sciences Database; Current Contents: Life Sciences; Index Medicus/MEDLINE; Journal Citation Reports/Science Edition; MEDLINE; PubMed Dietary Supplement Subset; Science Citation Index; Science Citation Index Expanded; SCOPUS; VINITI; Web of Science; Zoological Record. View this journal online at wileyonlinelibrary.com/journal/jmor

Wiley's Corporate Citizenship initiative seeks to address the environmental, social, economic, and ethical challenges faced in our business and which are important to our diverse stakeholder groups. Since launching the initiative, we have focused on sharing our content with those in need, enhancing community philanthropy, reducing our carbon impact, creating global guidelines and best practices for paper use, establishing a vendor code of ethics, and engaging our colleagues and other stakeholders in our efforts. Follow our progress at www.wiley.com/go/citizenship.

Disclaimer: The Publisher and Editors cannot be held responsible for errors or any consequences arising from the use of information contained in this journal; the views and opinions expressed do not necessarily reflect those of the Publisher and Editors, neither does the publication of advertisements constitute any endorsement by the Publisher and Editors of the products advertised.

Printed in Singapore by Markono Print Media Pte Ltd.

JOURNAL OF

morphology

Founded by C.O. Whitman, 1887
Originally Founded by the Wistar Institute

JOURNAL OF MORPHOLOGY 275:1238–1257 (2014)

Ultrastructure of Spermatozoa of Orsolobidae (Haplogynae, Araneae) With Implications on the Evolution of Sperm Transfer Forms in Dysderoidea

Elisabeth Lipke,[1*] Martín J. Ramírez,[2] and Peter Michalik[1,3]

[1]*Zoological Institute and Museum, Ernst-Moritz-Arndt University of Greifswald, J.-S.-Bach-Straße 11/12, Greifswald D-17489, Germany*
[2]*Research Scientist, Division of Arachnology, Museo Argentino de Ciencias Naturales—CONICET, Buenos, Aires, Argentina*
[3]*Research Associate, Division of Invertebrate Zoology, American Museum of Natural History, New York*

ABSTRACT Haplogynae are highly diverse with respect to the primary male genital system and sperm characteristics. Additionally, all sperm transfer forms (STF) known for spiders are present. Besides individually transferred sperm (cleistospermia), sperm are transferred as conjugates, both primary (synspermia) and secondary sperm conjugates (coenospermia, rouleaux) occur. Nevertheless, the ultrastructure of spermatozoa and STF are described for few Haplogynae and often only one representative species was studied, resulting in a superficial insight in the evolution of these traits. To elucidate the evolution of STF within Haplogynae we investigated representatives of four genera of the dysderoid family Orsolobidae. Our data show the presence of synspermia (*Orsolobus*, *Osornolobus*, *Hickmanolobus*, and *Tasmanoonops*) and also cleistospermia (*Osornolobus*). The occurrence of different STF within one family or even genus has not been described for any other spider taxon so far. Moreover, the synspermia of species of *Tasmanoonops* and *Hickmanolobus* were not covered by a secretion sheath suggesting a previously unknown strategy of transferring sperm that is possibly related to sperm residency time or female triggered processes after copulation. Based on serial ultrathin sectioning and subsequent 3D-reconstruction, we obtained detailed measurements revealing remarkable size differences of STF. To evaluate the previously suggested correlation with the most distal region of the spermophor inside the embolus (intromittent part of the copulatory organ) we measured the diameter of the spermophor using micro-computed X-ray tomography data to obtain corresponding morphometric parameters. Based on these data only two species show similarity in STF and spermophor diameter. J. Morphol. 275:1238–1257, 2014. © 2014 Wiley Periodicals, Inc.

KEY WORDS: 3D-reconstruction; cleistospermia; synspermia; palpal organ; micro-computed X-ray tomography

INTRODUCTION

Sperm show a remarkably high morphological diversity and are phylogenetically informative (e.g., Jamieson, 1987; Pitnick et al., 2009). As a result of sexual selection and sperm competition, sperm are maximized in number while minimized in size (Arnaud et al., 2001). Throughout numerous taxa, the same selective forces likely provoked the occurrence of giant, as well as conjugated sperm (e.g., Afzelius and Dallai, 1987; Briskie et al., 1997; LaMunyon and Ward, 2002; Hosken, 2003; Higginson et al., 2012b). Sperm conjugation is rare, but present in a variety of animal taxa including mammals, arthropods, and mollusks (Higginson and Pitnick, 2011). Two different types of sperm conjugation can be distinguished (Higginson and Pitnick, 2011). Primary sperm conjugates derive from a common spermatogonium and remain grouped together, whereas secondary sperm conjugates are formed after sperm cell separation during spermiogenesis (Higginson and Pitnick, 2011).

In spiders, both types of sperm conjugation are present. Moreover, spider spermatozoa are always transferred in a coiled and encapsulated condition (see, Alberti, 1990; Michalik and Lipke, 2013). Among spiders, Haplogynae are one of the most morphologically diverse groups and phylogenetically not well understood (Ramirez, 2000). Moreover, in addition to complex male and female

Additional Supporting Information may be found in the online version of this article.

Contract grant sponsor: German Research Foundation; Grant number: DFG Mi 1255/5-1 (P.M.).

*Correspondence to: Elisabeth Lipke; General Zoology and Zoological Systematics, Zoological Institute and Museum, Ernst-Moritz-Arndt University of Greifswald, Anklamer Str. 20, D-17489 Greifswald, Germany. E-mail: ELipke@gmx.de

Received 23 January 2014; Revised 15 May 2014;
Accepted 16 May 2014.

Published online 3 June 2014 in
Wiley Online Library (wileyonlinelibrary.com).
DOI 10.1002/jmor.20298

genitalia of some Pholcidae and Oonopidae (e.g., Huber and González, 2001; Huber, 2005, 2006; Huber et al., 2005; Burger et al., 2006, 2010; Burger, 2010, 2011), Haplogynae show an astonishing diversity of their sperm transfer forms (STF) and all types of STF known for spiders are present (reviewed in e.g., Alberti, 1990; Michalik and Lipke, 2013).

As indicated by the few studies dealing with the relationships of this spider group, the cribellate Filistatidae is sister to the ecribellate Haplogynae—with Dysderoidea and Scytodoidea as main taxa—(Platnick et al., 1991; Ramirez, 2000). The taxon Dysderoidea consists of four families (Segestriidae, Dysderidae, Orsolobidae, and Oonopidae) and is the sister group to the small family Caponiidae (Platnick et al., 1991, Ramirez, 2000). Based on few data available from literature, secondary sperm conjugates (coenospermia) are known from Filistatidae, whereas in Dysderoidea representatives of Segestriidae and Dysderidae transfer primary sperm conjugates (synspermia) (Alberti and Weinmann, 1985; Michalik et al., 2004a). Individually transferred sperm (cleistospermia) are described for a representative of Oonopidae (Alberti and Weinmann, 1985). However, due to the limited taxon sampling and missing data of several families the evolution of STF is still not understood.

The present study focusses on the primary male reproductive system and STF of Orsolobidae for the first time. Our study aims to (1) reveal the STF for this dysderoid taxon and (2) conceptualize characters of spermatozoa and primary male genital system with regard to their implications especially in the context of debated relationships of Dysderoidea and Haplogynae. Moreover, we generated comprehensive morphometric data of STF and corresponding male copulatory organs to gain evidence for a previously suggested correlation.

MATERIALS AND METHODS

Studied Species

Orsolobus pucara Forster and Platnick, 1985. 1 ad ♂ [FML-7]: Parque Nacional Huerquehue (Laguna Toro), Cautín, Reg. IX, Chile (S 39° 08′ 18.7″ W 71° 42′ 30.9″, 995 m, 7.02.2005; leg. F. Labarque, M. J. Ramírez).

Osornolobus sp. 1 (undescribed sp., near O. canan, or O. chiloe). 3 ad ♂ [PM-0036]/ [PM-0037]/ [PM-0038]: Parque Nacional Chiloé (Sendero Tepual, near Cucao), Chiloé, Chile (S 42.61766°, W 74.10120°, 15 m, 15.02.2012; leg: K. Huckstorf, M. Izquierdo, P. Michalik, M. J. Ramírez, C.S. Wirkner)

Osornolobus sp. 2 (undescribed sp., near O. thayerae). 1 ad ♂ [PM-0047]: Lago Huillinco (opposite site of Cabanas Puquelahue), Chiloe, Chile (S 42.66398°, W74.01012°, 3m, 16.02.2012; leg.: K. Huckstorf, M. Izquierdo, P. Michalik, M. J. Ramírez, C. S. Wirkner).

Tasmanoonops alipes. 1 ad ♂ [PM-0175]: Mount Wellington Park (trail to Organ Pipes "The Chalet"), Tasmania, Australia (S 42°53.418′, E 147°14.167′; 1027m; 20.02.2013; leg.: M. J. Ramírez, P. Michalik).

Tasmanoonops sp. 1 (undescribed sp.). 1 ad ♂ [PM-0143]: Barrington Tops National Park (Devil's hole; path to lookout), New South Wales, Australia (S 31°55′04.6″, E 151°29′05.7″; 1386 m; 04.02.2013; leg.: M. Ramírez, P. Michalik).

Tasmanoonops sp. 2 (undescribed sp., near T. complexus). 1 ad ♂ [PM-0209]: Barrington Tops National Park (Honeysuckle Trail), New South Wales, Australia (S 31°54′03.1″, E 151°32′01.7″, 1311 m, 03.02.2013; leg.: M. J. Ramírez, P.Michalik).

Hickmanolobus mollipes (Hickman, 1932). 1 ad ♂ [PM-0159]: Barrington Tops National Park (Honeysuckle Trail), New South Wales, Australia (S 31°54′03.1″, E 151°32′01.7″, 1311 m, 03.02.2013; leg.: M. J. Ramírez, P.Michalik).

Vouchers are deposited in the Zoological Museum of the University of Greifswald.

Species identifications were made by comparing standard diagnostic characters (mainly male copulatory organ) with the recent taxonomic revisions of Forster and Platnick (1985), the original descriptions (Hickman, 1932; 1979; Baehr and Smith, 2008; Baehr et al., 2011) and reference material identified in the Museo Argentino de Ciencias Naturales. Undescribed species were detected and discriminated by diagnostic differences in male genitalia; the family is under review by Tamas Szuts and Charles Griswold (California Academy of Sciences, San Francisco), who confirmed that there are numerous undescribed species in those genera; we will make our specimens available for their taxonomic revision.

Histology

Males were dissected either in the field or the lab in 0.1 M phosphate buffer (PB) to which 1.8% sucrose was added. Isolated reproductive systems were then fixed in 2.5% glutaraldehyde in PB and further processed in the lab at University of Greifswald. Documentation of the gross morphology was performed using a Zeiss Discovery V20 stereo microscope with a Zeiss MCr camera. The tissue was postfixed in PB buffered 2% OsO_4. After being washed in PB, it was dehydrated in graded ethanol and embedded in Spurr's resin (Spurr, 1969). Serial semithin sections (700 nm) were obtained using a Diatome Ultra 45° diamond knife on a Leica ultramicrotome UCT and finally stained according to Richardson et al. (1960).

Transmission Electron Microscopy

Ultrathin sections (70 nm), as well as serial-ultrathin sections (60 nm) were cut with a Diatome diamond knife on a Leica ultramicrotome UCT and either applied to copper mesh-grids or slot-grids (Science Services), covered with a thin layer of desiccated pioloform solution (1% Pioloform in 100% chloroform). Postprocessing included staining with uranyl acetate and lead citrate according to Reynolds (1963). Finally sections were examined using (1) a JEOL JEM 1011 electron microscope equipped with an Olympus Mega View III digital camera at 80 kV and (2) a Carl Zeiss EM 902, equipped with a Proscan digital camera.

Micro-computed X-ray Tomography (μCT)

Micro-computed X-ray tomography scans of the palps were performed using an XRadia Micro XCT-200 (Carl Zeiss X-ray Microscopy). Samples were dehydrated in graded ethanol (80 and 90%, pure ethanol) and stained in 1% iodine solution (in pure ethanol) overnight. Samples were then placed in small container glued on an insect pin, filled with a small amount of petrol jelly and pure ethanol. A summary of all μCT-settings and corresponding voucher identities is given in Supporting Information Table 1. Tomography projections were reconstructed using the reconstruction software provided by XRadia.

TABLE 1. MorphDBase links at which image stacks obtained by μCT and serial section TEM that are used for the reconstruction of the male palpal organ and sperm transfer forms are stored

	MorphDBase link	
Species	palp (μCT image stack)	sperm transfer form (serial TEM images)
Orsolobus pucara	https://www.morphdbase.de?E_Lipke_20140117-M-23.1	https://www.morphdbase.de?E_Lipke_20140107-M-20.1
Osornolobus sp. 1	https://www.morphdbase.de?E_Lipke_20140117-M-24.1	https://www.morphdbase.de?E_Lipke_20140107-M-17.1
Osornolobus sp. 2	https://www.morphdbase.de?E_Lipke_20140117-M-29.1	https://www.morphdbase.de?E_Lipke_20140107-M-15.1
Tasmanoonops alipes	https://www.morphdbase.de?E_Lipke_20140117-M-28.1	https://www.morphdbase.de?E_Lipke_20140107-M-16.1
Tasmanoonops sp. 1	https://www.morphdbase.de?E_Lipke_20140117-M-26.1	https://www.morphdbase.de?E_Lipke_20140107-M-21.1
Tasmanoonops sp. 2	https://www.morphdbase.de?E_Lipke_20140117-M-25.1	https://www.morphdbase.de?E_Lipke_20140107-M-19.1
Hickmanolobus mollipes	https://www.morphdbase.de?E_Lipke_20140117-M-27.1	https://www.morphdbase.de?E_Lipke_20140107-M-18.1

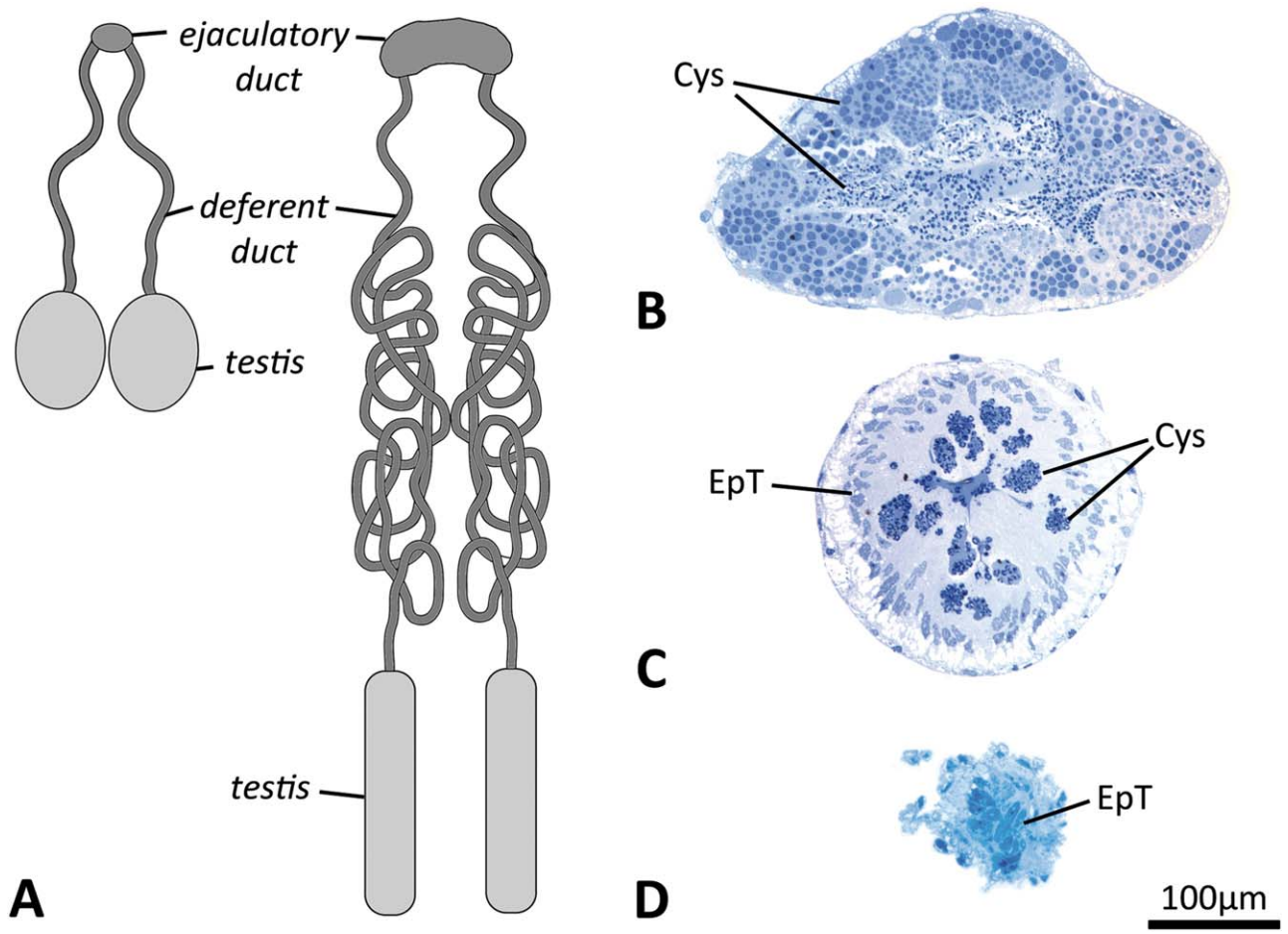

Fig. 1. Organization of the primary male reproductive system. **A**: Schematic drawing of the primary reproductive system of *Hickmanolobus mollipes* (left) with oval testes and short deferent ducts that join distally, forming the ejaculatory duct. All remaining investigated orsolobids (*Orsolobus pucara*, *Osornolobus* sp. 1, *Osornolobus* sp. 2, *Tasmanoonops alipes*, *Tasmanoonop*s sp. 1, and *Tasmanoonops* sp. 2) show paired, elongated testes and very long convoluted deferent ducts that fuse to form the ejaculatory duct. **B**: Cross-section of the testis of *Osornolobus* sp. 2 with cysts of developing sperm of different spermatogenic stages. **C**: Cross-section of the testis of *Osornolobus* sp. 1 indicating the absence of early spermatogenic stages. Within cysts, only late, almost mature spermatids are visible. **D**: Cross-section of the testis of *Tasmanoonops* sp. 1 showing only somatic cells and a stretched basal lamina. Cys, cyst of developing sperm; EpT, epithelium of testis.

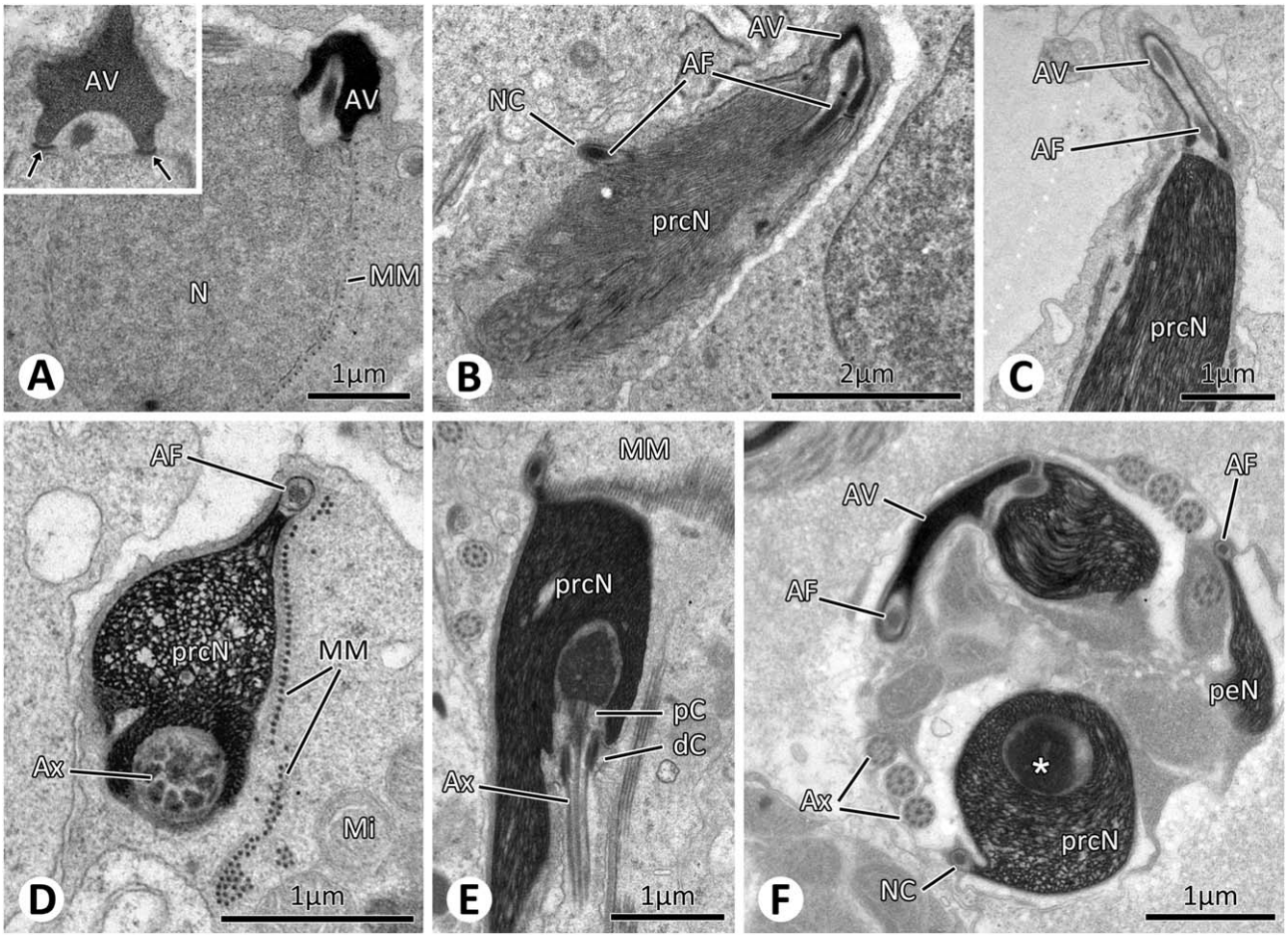

Fig. 2. Spermiogenesis of *Osornolobus* sp. 2, exemplified for all orsolobids. **A**: Early stages of spermatogenesis are characterized by a spherical nucleus, surrounded by a distinct "manchette of microtubules." At the anterior pole the acrosomal complex (AV and AF) is formed. Note the small electron dense border (arrows), separating the AV from the nucleus. **B**: In midspermatids the nucleus enlarges and therefore reduces its size. **C**: The AV narrows while simultaneously enlarging, resulting in the final cylindrical, or conical shape, respectively. **D**: Late spermatids are characterized by condensed chromatin that retains some electron lucent areas. The distal centriole and base of the axoneme are surrounded by little electron dense material, forming a centriolar adjunct. **E**: The short but wide implantation fossa contains the two centrioles, the base of the axoneme and electron dense material. Note little electron dense material around the distal centriole. **F**: At the end of spermiogenesis the sperm coil. Note electron dense material within the implantation fossa (asterisks). AF, acrosomal filament; AV, acrosomal vacuole; Ax, axoneme; dC, distal centriole; Mi, mitochondria; MM, manchette of microtubules; N, nucleus; NC, nuclear canal; peN, postcentriolar elongation of nucleus; prcN, precentriolar portion of nucleus.

3D-Reconstruction and Measurements

For the 3D-reconstruction of depicted synspermia and cleistospermia we used series of ultrathin sections, obtained from the distal deferent ducts, near the genital opening. For the alignment and successive segmentation of cell components, Amira 5.4.5 (FEI, Visualization Science Group) was used. In addition, serial sections of *Tasmanoonops* sp. 1 were aligned elastically using the Fiji plugin TrakEM2 (according to Saalfeld et al., 2012), before further processed in Amira 5.4.5. In each section, contours of the main cell components were delineated manually. The obtained labels were then interpolated to keep the refinement of structures and a 3D surface was generated. Further processing was performed using the surface editor for refining the surface as a whole, as well as the smooth surface function. We implemented the 3D models into pdf files using Adobe Acrobat Pro Extended (Adobe Systems). Measurements were performed using "CenterlineTree" function of the skeleton pack and "surface area" function of Amira 5.4.5. The volume as well as total length of each cell component was then used to calculate the natural length by means of the pixel/µm ratio (voxel/μm^3, based on the scale of the TEM section). Measurements were performed on at least two synspermia or cleistospermia for each specimen, length and volumes are given as a mean value.

Image stacks obtained by µCT were used to visualize and measure the spermophor and embolus inside the male palpal organ. Therefore, contours as well as the lumen were encircled, the resulting Labelfield was resampled and a surface was generated using the "SurfaceGen" function. Postprocessing included "SurfaceEditor" and the "SmoothSurface" function. Finally, obtained surfaces were visualized with a volume reconstruction of the whole tarsal segment of the pedipalps using the "Volren" function. Colormaps were set to "VolrenGlow" and the histograms were adjusted to individual image stack qualities.

The image stacks (tiff-images) used for volume rendering of the palpal organs and segmentation of the spermophor, as well as STF obtained by serial section TEM, are deposited in MorphDBase (see Table 1).

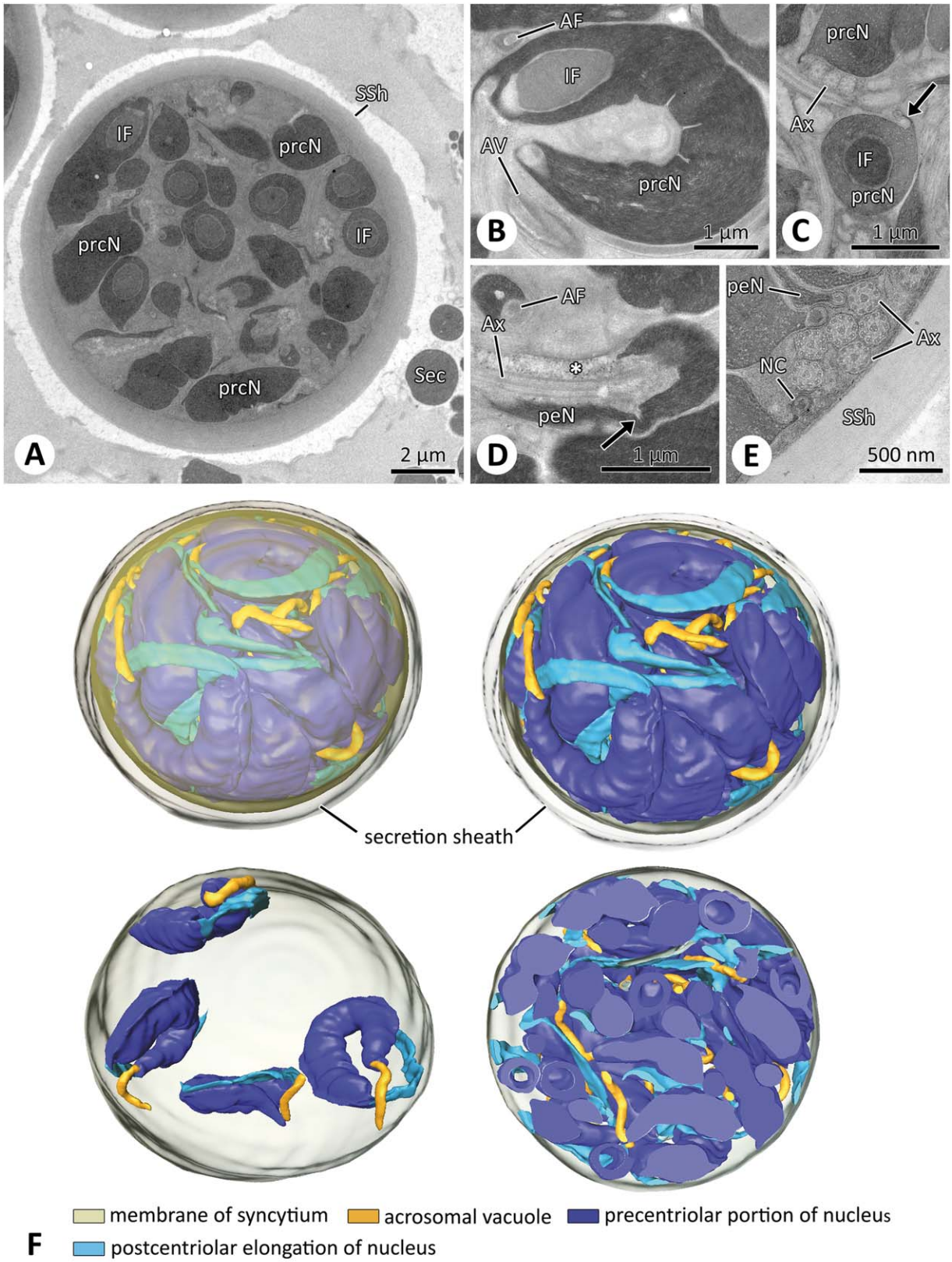

Fig. 3. Characteristics of mature spermatozoa and 3D-reconstruction of STF of *Orsolobus pucara*. **A**: Synspermia of *O. pucara* contain either 16, or 32 individual sperm, resulting in large sperm conjugates. **B**: The compact precentriolar portion of the nucleus is characterized by a wide implantation fossa that is filled with a distinct centriolar adjunct. **C**: Characteristic for *O. pucara*, the NC is situated on a distinct crest, thus appears stalked (arrow). **D**: The postcentriolar elongation starts with an indentation (arrow), the base of the axoneme is surrounded by a distinct amount of glycogen (asterisks). **E**: A thick, multilayered secretion sheath surrounds the sperm conjugate. **F**: Reconstruction of an entire synspermium comprising 32 individual sperm. These sperm are coiled and densely packed in the synspermium. Parts of the sperm (axoneme, AF, and NC) are not visualized. AF, acrosomal filament; AV, acrosomal vacuole; Ax, axoneme; IF, implantation fossa; NC, nuclear canal; peN, postcentriolar elongation of nucleus; prcN, precentriolar portion of nucleus; Sec, secretions; SSh, secretion sheath.

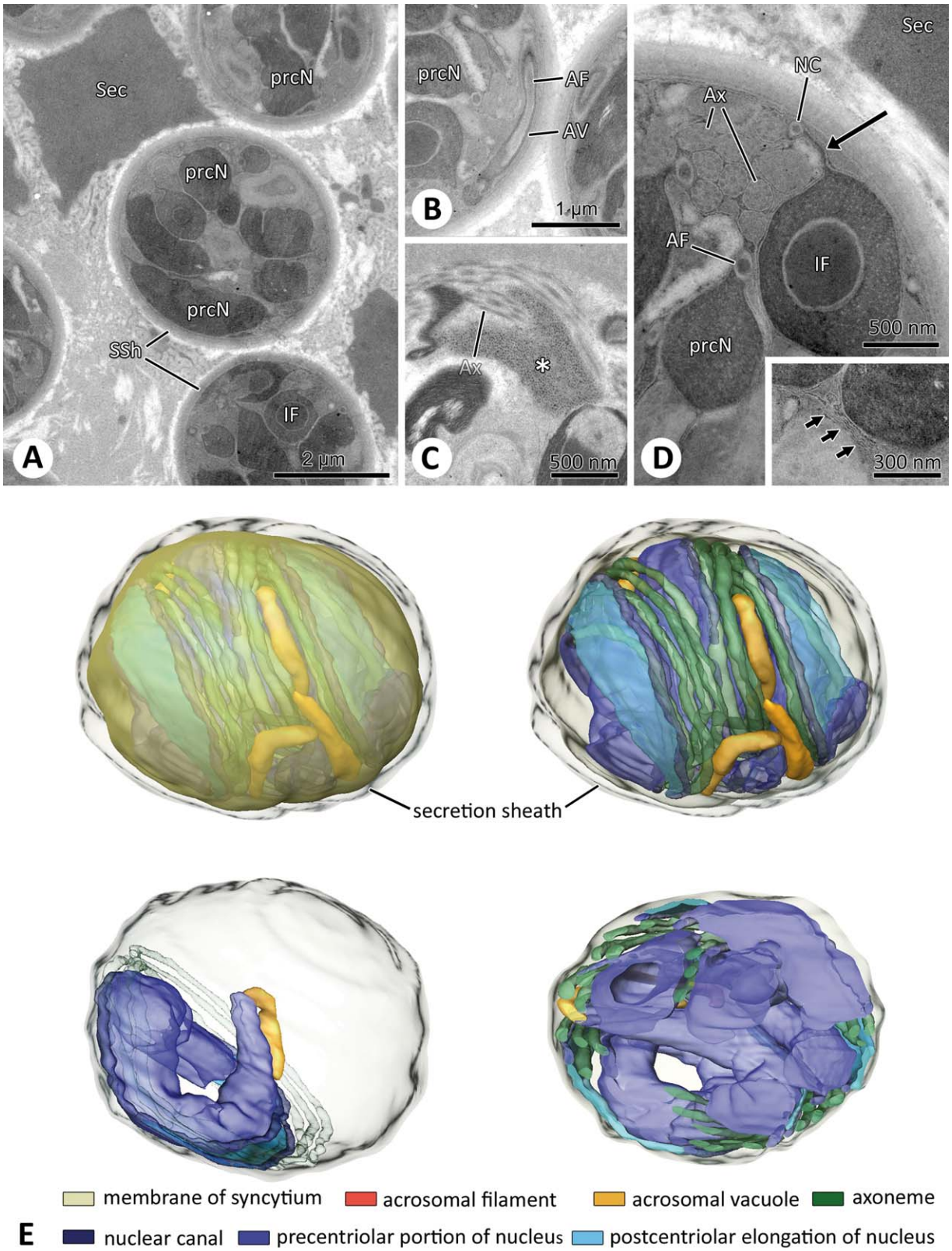

Fig. 4. Characteristics of mature spermatozoa and 3D-reconstruction of STF of *Osornolobus* sp. 1. **A**: The deferent duct is filled with numerous synspermia, as well as large, electron dense secretions that appear rectangular. **B**: The long, cylindrical AV is located in the periphery of the sperm conjugate. **C**: A large amount of granules, certainly glycogen is present alongside the base of the axoneme (asterisk). **D**: Several cross-sections of the coiled axonemes are visible. The NC is stalked (arrow) a. Among individual spermatozoa pronounced membrane stacks are visible (inset, arrows). **E**: 3D-reconstruction of an entire synspermium (PM-0038), indicating the arrangement of four fused spermatozoa and their cell components within the sperm conjugate. AF, acrosomal filament; AV, acrosomal vacuole; Ax, axoneme; IF, implantation fossa; Mv, microvilli; NC, nuclear canal; peN, postcentriolar elongation of nucleus, prcN, precentriolar portion of nucleus; Sec, secretions; SSh, secretion sheath.

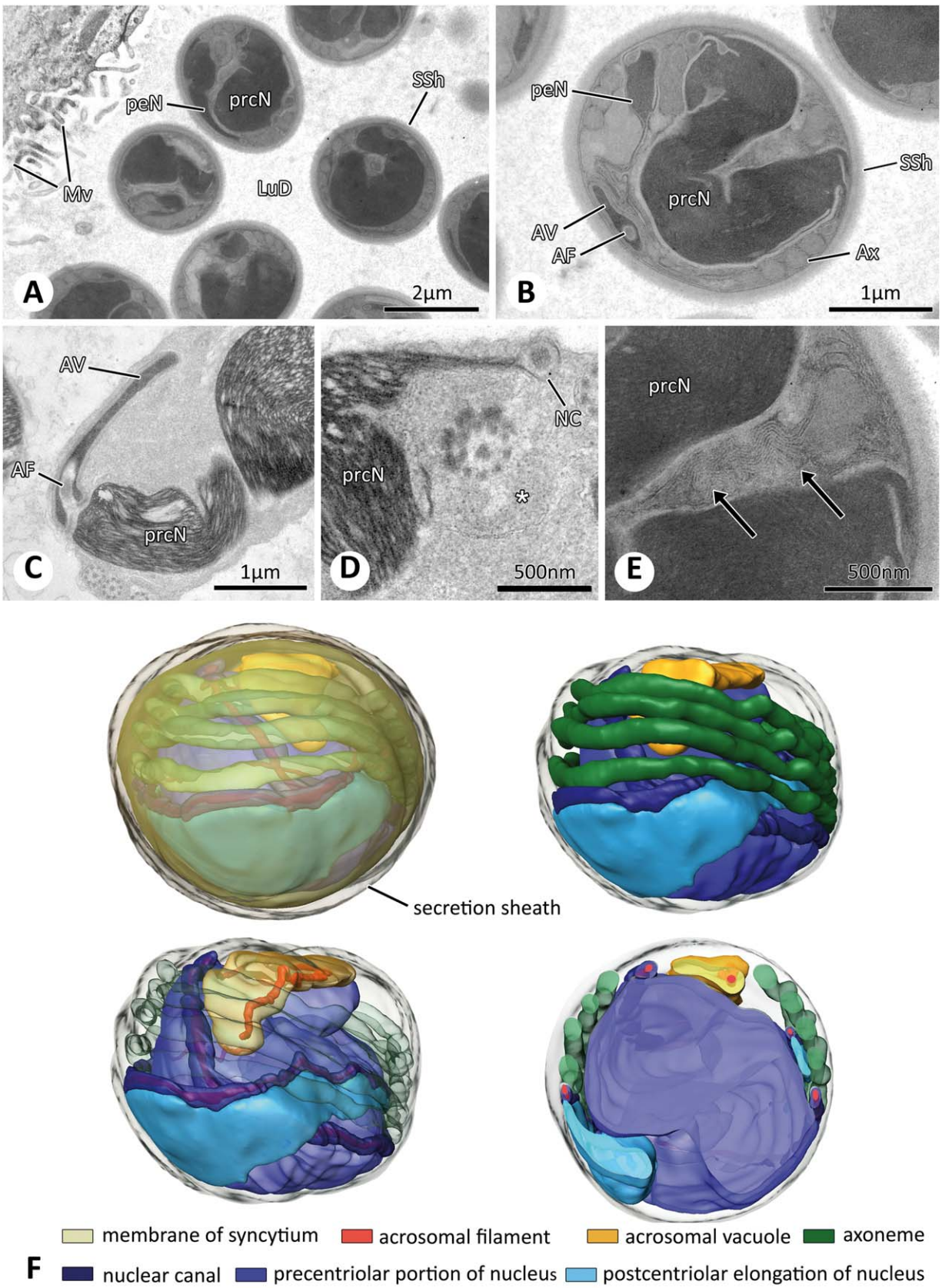
A
peN
prcN
SSh
Mv
LuD
2µm
B
peN
SSh
prcN
AV
AF
Ax
1µm
C
AV
AF
prcN
1µm
D
NC
prcN
500nm
E
prcN
500nm
secretion sheath
F
membrane of syncytium
acrosomal filament
acrosomal vacuole
axoneme
nuclear canal
precentriolar portion of nucleus
postcentriolar elongation of nucleus

Fig. 5.

RESULTS

Primary Male Reproductive System

The primary male reproductive system of all investigated orsolobid species, except *Hickmanolobus mollipes*, consists of two elongated testes and long, convoluted deferent ducts (Fig. 1A). These deferent ducts fuse at their distal portions, forming the unpaired ejaculatory duct (Fig. 1A). In contrast, testes of *H. mollipes* are oval (Figs. 1A,B), and the deferent ducts are rather short. Testical cross-sections of *H. mollipes* and *Osornolobus* sp. 2 reveal the typical organization for spiders. Somatic cells surround cysts of germ cells (Fig. 1B). Each cyst contains germ cells of the same developmental stage. Early spermatogenic stages are mostly located in the periphery, whereas the lumen of the testis bears almost mature spermatozoa and sperm conjugates. In contrast, only late spermatids were found in representatives of *Osornolobus* sp. 1 (Fig. 1C), *Tasmanoonops alipes*, and *Tasmanoonops* sp. 2, indicating a synchronous spermatogenesis. Neither spermatogenic stages, nor spermatids were found in *Tasmanoonops* sp. 1 (Fig. 1D). Here, cross-sections revealed only somatic cells and a thick basal lamina (Fig. 1D).

Spermiogenesis

Although there is only evidence from two orsolobid species (*H. mollipes* and *Osornolobus* sp. 1), we assume spermiogenesis follows the same pattern in the remaining orsolobid species. Early spermatids that are derived from spermatogonia by meiotic divisions are mainly characterized by their large spherical nucleus, which is surrounded by a so-called manchette of microtubules (Fig. 2A), mitochondria, centrioles, and Golgi apparatus. Vesicles that are derived from the Golgi apparatus fuse to form an early stage of the acrosomal vacuole (AV) at the anterior pole of the nucleus (Fig. 2A). Subsequently, the AV enlarges, forming a subacrosomal space, where the acrosomal filament (AF) originates (Figs. 2A,B). The AV is separated from the nucleus by a distinct electron dense plate (Figs. 2A,F). Simultaneously, the two centrioles migrate toward the posterior pole of the nucleus, resulting in the so-called implantation fossa, an indentation of the latter. In mid spermatids, the nucleus elongates while the chromatin begins to condense and appears fibrillar (Figs. 2B,C). The nuclear canal (NC) that runs in the periphery of the nucleus contains the AF (Figs. 2D–F).

Late spermatids are characterized by an elongated AV, highly condensed chromatin, a compact, cylindrical precentriolar portion of nucleus and a distinct asymmetrical postcentriolar elongation of nucleus. Finally, main cell components (nucleus and axoneme) coil (Fig. 2F) while the manchette of microtubules disintegrates.

Mature Spermatozoa

In general, the spermatozoa are characterized by the characteristics described below (see also Table 2). If not especially mentioned, these characteristics were equally found in all investigated species. The main sperm cell components of all investigated orsolobid species are additionally depicted in interactive 3D-reconstructions (Figs. 3–9).

Acrosomal complex—AV: cylindrical in *O. pucara* and *Osornolobus* sp. 1, conical and flattened in all remaining taxa; narrow subacrosomal space (Figs. 4B, 5C, 6A,C–D, 7A, 8B, and 9B); long (N to AV ratio 2:1) in *Osornolobus* sp. 2, all *Tasmanoonops* species (*T. alipes*; *Tasmanoonops* sp. 1 and *Tasmanoonops* sp. 2) and *H. mollipes*, shorter in *O. pucara* (N to AV ratio 3:1) and *Osornolobus* sp.1 (N to AV ratio 4:1); AF: extends within the NC into the postcentriolar elongation, ends shortly before the end of NC (e.g., Figs. 3E, 7A, 8E, and 9C,D).

Nucleus (N)—precentriolar region of nucleus (prcN) compact and nearly cylindrical in all investigated species (compare interactive 3D-reconstructions). The postcentriolar elongation (peN) starts with a crest before it extends (Figs. 3D, 7C, and 9E). peN is as long as prcN in *O. pucara*, *Osornolobus* sp. 2, *H. mollipes*, *Tasmanoonops* sp. 1 and *Tasmanoonops* sp. 2. peN is shorter than prcN in *Osornolobus* sp. 1 (peN to prcN ratio 1:2) and *Tasmanoonops* sp. 2 (peN to prcN ratio 1:1.5). The NC runs peripherally (Figs. 6A and 8A), and appears stalked on a small ridge in the posterior portion of the prcN in *O. pucara*, *Osornolobus* sp. 1, *Osornolobus* sp. 2, and *H. mollipes* (Figs. 3A–C, 4D, 5B, and 9C,D). The wide, but usually small implantation fossa (compare 3D-reconstructions), contains the two centrioles, the base of the axoneme and is filled with electron dense material (Figs. 3A–C, 4D, 6D, 7A, 8C, and 9C,E), forming an electron-dense centriolar adjunct.

Axoneme (Ax)—9 + 3 microtubular pattern (e.g., Figs. 3E, 4D, 6E, 7B, 8D, and 9D). The axoneme is always longer than the nucleus (prcN + peN).

Fig. 5. Characteristics of mature spermatozoa and 3D-reconstruction of STF of *Osornolobus* sp. 2. **A**: Numerous cleistospermia can be identified in the lumen of the deferent ducts, each surrounded by a secretion sheath. **B**: Individual sperm demonstrating the compact arrangement of sperm cell components. **C**: The long AV contains the AF. **D**: The NC is placed on a distinct crest alongside the proximal part of the precentriolar portion of nucleus. Note small amount of glycogen (asterisks) that is present around the base of the axoneme. **E**: Membrane stacks are visible among coiled cell components (arrows). **F**: 3D-reconstruction showing the coiled axoneme, surrounding all main cell components. AF, acrosomal filament; AV, acrosomal vacuole; Ax, axoneme; LuD, lumen of deferent duct; Mv, microvilli; NC, nuclear canal; peN, postcentriolar elongation of nucleus; prcN, precentriolar portion of nucleus; SSh, secretion sheath.

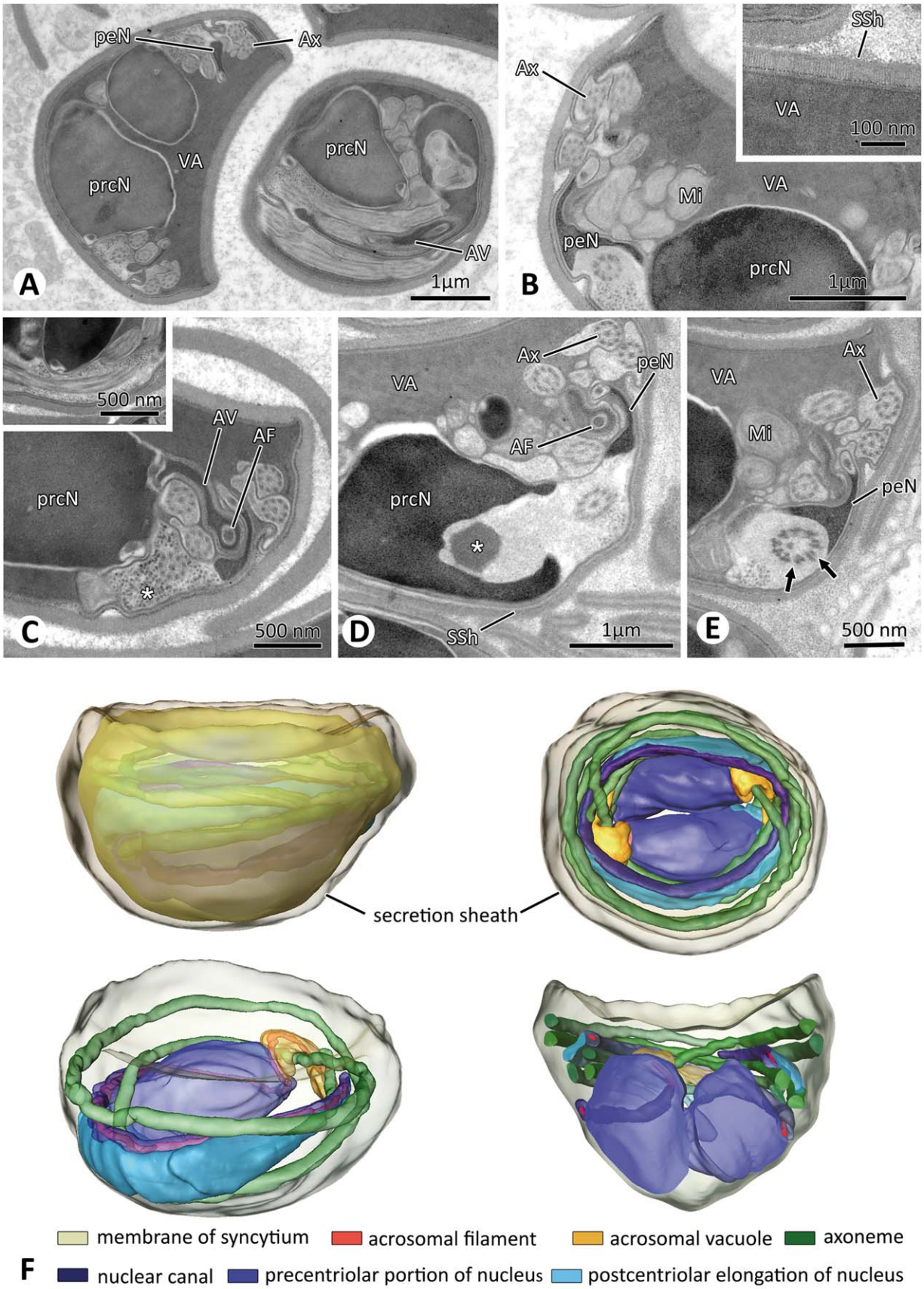
peN
Ax
VA
prcN
prcN
AV
1µm
A
Ax
SSh
VA
100 nm
Mi
VA
peN
prcN
1µm
B
500 nm
AV
AF
prcN
*
500 nm
C
Ax
peN
VA
AF
prcN
*
SSh
1µm
D
Ax
VA
Mi
peN
500 nm
E
secretion sheath
membrane of syncytium
acrosomal filament
acrosomal vacuole
axoneme
F
nuclear canal
precentriolar portion of nucleus
postcentriolar elongation of nucleus

Fig. 6.

There are short central tubuli in *Tasmanoonops* sp. 2 (Figs. 8D–E). The distal centriole is always surrounded by some electron dense material (e.g., Figs. 5D, 6E, 7C, and 9E).

Cell inclusions—Mitochondria are always present within the cytoplasm. A distinct amount of glycogen is always present around the base of the axoneme and along the base of the peN (Figs. 3D, 4C, 5D, 6C,D, 7D, 8D–E, and 9E). A distinct vesicular area is present in *Tasmanoonops* species (*T. alipes*, *T.* sp. 1, *T.* sp. 2) and *H. mollipes* (Figs. 6A–E, 7A,B, 8A–E, and 9A–D), but absent in both *Osornolobus* species, as well as in *O. pucara*. If present, the vesicular area appears compact and is electron dense in all three *Tasmanoonops* species, but more electron lucent in *H. mollipes*.

Sperm Transfer Forms

All orsolobid species except *Osornolobus* sp. 2 possess synspermia as their STF (Figs. 3A, 4A, 6A, 7A, 8A, and 9A). Most of these primary sperm conjugates consist of two (*T. alipes, Tasmanoonops* sp. 1, *Tasmanoonops* sp. 2, and *H. mollipes*), those of *Osornolobus* sp. 1 consist of four fused spermatozoa (Table 3). The large synspermia of *O. pucara* consists of either 16 or 32 fused sperm cells (Table 3). Fused sperm of primary conjugates originate from one cyst. Although all spermatids of all developmental stages remain connected with each other via cell bridges, the cell membranes of a certain number of spermatids (see number of fused sperm of investigated species) start to fuse along their entire length, while the main cell components coil. While the spermatids start to fuse, they combine their cytoplasm. As a consequence, the developing conjugate is rather large. Further development includes the reduction of the abundant cytoplasm and cell membranes.

Only in *Osornolobus* sp. 2 late spermatids do not fuse but separate after coiling. Here, individual coiled spermatozoa that are no longer connected by cellular bridges are released into the lumen of the testis (Figs. 5A,B).

Secretion Sheath

A secretion sheath of variable thickness is present in all investigated species except *Tasmanoonops* sp. 1 and *H. mollipes* where two fused spermatozoa are surrounded by their syncytial membrane (Figs. 7A,B, and 9A,D–E). Sperm conjugates of *T. alipes* have the thinnest secretion sheath (less than 100 nm, Fig. 6B, inset), the secretion sheaths of *Osornolobus* sp. 1, *Osornolobus* sp. 2, and *Tasmanoonops* sp. 2 are slightly thicker, ranging between 160 and 190 nm. In contrast, the large sperm conjugates of *O. pucara* have the thickest secretion sheath of ~450 nm (Figs. 3A,E), irrespective of size and number of sperm included in one sperm conjugate.

Male Copulatory Organs and Sperm Storage

The sperm duct (spermophor) in the palpal organ, the place where sperm cells are stored after uptake from the primary male genital system, opens usually at the tip of the embolus. It is a twisted, tube-like structure in *O. pucara*, *Osornolobus* sp. 1, and *Osornolobus* sp. 2 (Figs. 10B–D), and resembles a sac-like invagination in all three *Tasmanoonops* species (Figs. 10E–G). In *H. mollipes*, there is no embolus-like structure. Here, the short, tube-like spermophor opens near a small spine (Fig. 10H). In general, the spermophor is sclerotized, except of a small nonsclerotized portion in the distal part of the spermophor (Fig. 10A). Figure 11 summarizes the diameter of the distal spermophor at its thinnest point (DoS) and dimensions of transferred synspermia and cleistospermia for all analyzed species. Our data reveal an exceptionally wide DoS in *Tasmanoonops* sp. 1 of approx. 15 × 20 μm. This is surprising, as transferred synspermia are rather small (approx. 3.5 × 4 × 4 μm) and although lacking a secretion sheath are similar to those of *T. alipes* (4 × 4 × 4 μm), a species with a narrow DoS, half the size of the latter (approx. 7 × 10 μm). The DoS is rather narrow in those orsolobids transferring cleistospermia (*H. mollipes*) and small synspermia (*Osornolobus* sp. 2, *Tasmanoonops alipes* and *Tasmanoonops* sp. 2), whereas those transferring large synspermia, as *O. pucara*, provide a wide DoS.

DISCUSSION

Phylogenetic Implications

A comparison of relevant characters that are associated with the primary male genital system and sperm is given in Table 2. Within Dysderoidea

Fig. 6. Characteristics of mature spermatozoa and 3D-reconstruction of STF of *Tasmanoonops alipes*. **A**: Synspermia in the deferent ducts of *T. alipes*. Note sperm conjugates are not spherical but cup-shaped. **B**: Although thin, sperm conjugates are surrounded by a distinct secretion sheath of approximately 90 nm (inset). **C**: As in all other investigated orsolobids, glycogen is present alongside the base of the axoneme (inset). The AV is separated from the precentriolar portion of the nucleus by a distinct electron dense border. **D**: The conical and flattened AV is characterized by a narrow subacrosomal space that contains the AF. Note wide implantation fossa that is filled with electron dense material (asterisk). **E**: Little electron dense material surrounds the base of the axoneme (arrows). Mitochondria are always present. **F**: 3D-reconstruction of STF of *T. alipes* comprising two spermatozoa that are arranged opposed to each other. Sperm conjugates are provided with a moderate indentation, thus they appear cup-like. Note each AV bends around parts of the axoneme. AF, acrosomal filament; AV, acrosomal vacuole; Ax, axoneme; Mi, mitochondria; NC, nuclear canal; peN, postcentriolar elongation of nucleus; prcN, precentriolar portion of nucleus; VA, vesicular area.

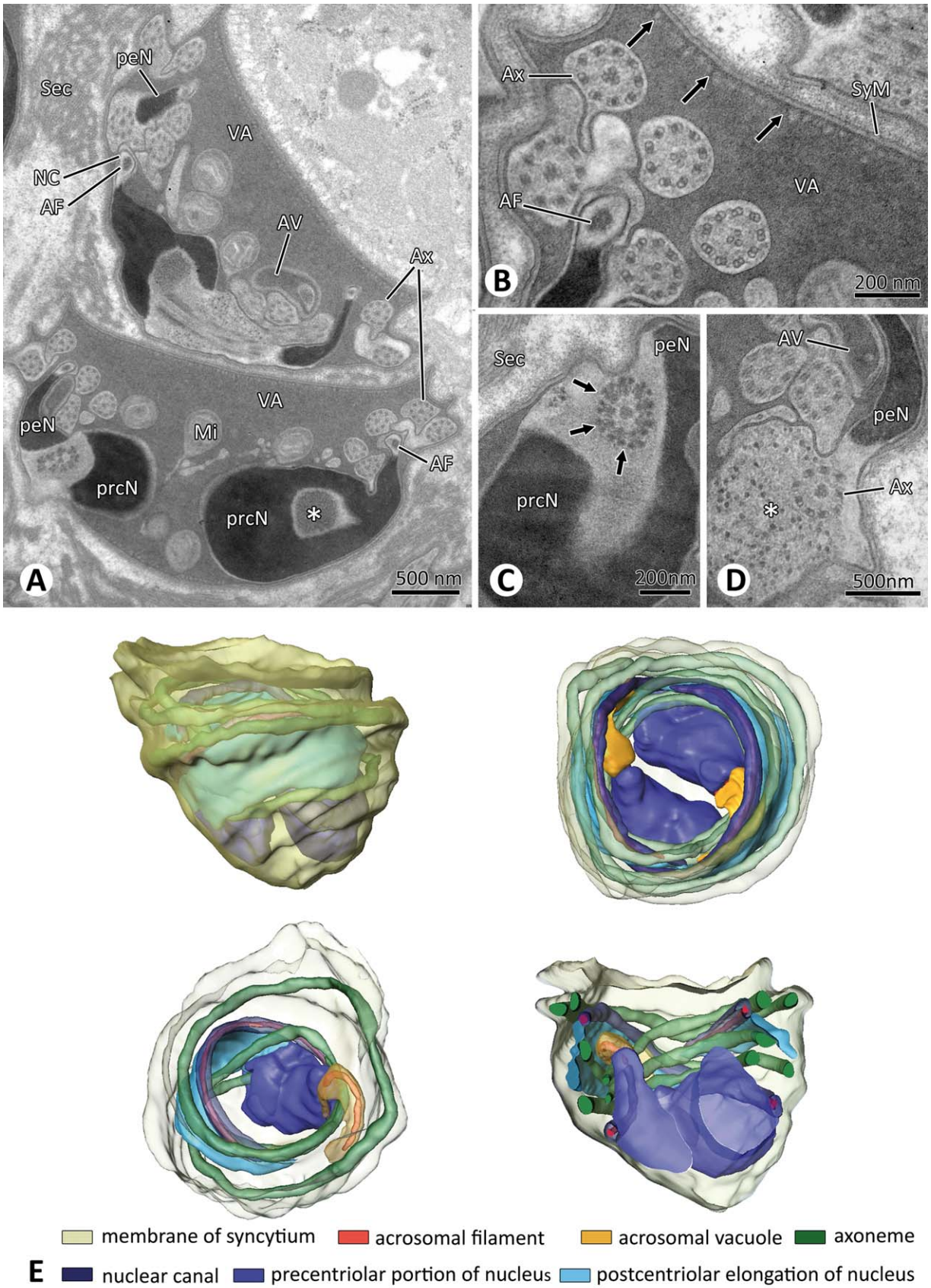
peN
Sec
VA
NC
AF
AV
Ax
VA
peN
Mi
AF
prcN
prcN
*
A
500 nm
Ax
SyM
AF
VA
B
200 nm
Sec
peN
prcN
C
200nm
AV
peN
Ax
*
D
500nm
membrane of syncytium
acrosomal filament
acrosomal vacuole
axoneme
E
nuclear canal
precentriolar portion of nucleus
postcentriolar elongation of nucleus

Fig. 7.

and Caponiidae, the gross morphology of the male genital system is diverse. Proximally fused testes are found in caponiids and dysderids (Michalik et al., 2004a; Lipke and Michalik, 2012), whereas completely fused testes are a synapomorphy for oonopids (Burger and Michalik, 2010). The organization of most orsolobids, with paired, elongated testes resembles that of segestriids and most other spider taxa, including mygalomorphs, basal araneomorphs, and entelegynes (Alberti et al., 1986; Alberti, 1990; Alberti and Coyle, 1991; Michalik, 2009; Michalik et al., 2013).

The spermophor of all investigated orsolobid taxa is provided with a small portion that appears less-sclerotized or nonsclerotized (Fig. 10). This condition is uncommon in spiders; so far only a few taxa are known with nonsclerotized spermophors, for example, Austrochilinae (Griswold et al., 2005; Michalik and Ramirez, 2013), or with their spermophor entirely devoid of a cuticular lining, a synapomorphy of Oonopinae (Burger, 2010). Orsolobidae plus Oonopidae were suggested to be sister groups within Dysderoidea (Platnick et al., 1991; Ramirez, 2000), but the unsclerotized section found in orsolobids is unlikely homologous to the one found in derived oonopines, because the two consecutive outgroups of oonopines (Orchestininae and Sulsulinae) have normally sclerotized spermophores (Platnick et al., 2012).

Our data show that spermatozoa of Orsolobidae share many characters known from Dysderidae as, for example, the shape and length of the AV (in relation to the nucleus) and the peculiar crest from which the postcentriolar elongation extends. These characters were only described for representatives of Dysderidae so far (Alberti and Weinmann, 1985; Michalik et al., 2004a) and suggest that dysderids and orsolobids might be more closely related than they were considered before. Besides, our results reveal some characters such as a distinct area of glycogen, surrounding the axonemal base that are depicted in several spider taxa (Alberti and Weinmann, 1985; Alberti and Coyle, 1991; Michalik et al., 2003; Michalik et al., 2004a; Lipke and Michalik, 2012) and likely reflect the plesiomorphic condition in spiders.

The peculiar axoneme of *Tasmanoonops* sp. 2 with its very short central tubuli likely affects the motility pattern. Nevertheless, the axoneme of *Tasmanoonops* sp. 2 reflects the typical organization of a spider axoneme (9 + 3 axonemal pattern, Dallai et al., 1995) and is certainly not comparable to the derived 9 + 0 axonemal pattern present in Pimoidae and Linyphiidae (Michalik and Alberti, 2005; Michalik and Hormiga, 2010).

Among the investigated Orsolobidae, we could identify a common morphology of sperm conjugates, unifying all investigated *Tasmanoonops* species. In contrast to the usually spherical shaped STF of most spider taxa, the shape of these synspermia appears cup-like (*T. alipes*), twisted (*Tasmanoonops* sp. 2) or both (*Tasmanoonops* sp. 1).

Evolutionary and Functional Implications

Primary male reproductive system. The histological analysis of the testis of adult males of some specimens showed (i) a comparable small testis volume and only one spermatogenic stage in *Osornolobus* sp. 1, *T. alipes*, *Tasmanoonops* sp. 2, and (ii) the absence of generative tissue in *Tasmanoonops* sp. 1. Nevertheless, STF are abundantly present in the lumen of the deferent ducts of all investigated specimens. Thus, the production of sperm in these species might be terminated as recently suggested for the Tasmanian cave spider, *Hickmania troglodytes* (Austrochilidae) (Michalik et al., 2014). However, because we do not have a reasonable sample size and cannot exclude age or teratological effects no further conclusions can be drawn. Future studies should address a potential sperm limitation by termination of spermiogenesis in early adult stage in Orsolobidae especially with regard to mating strategies. As shown for some orbicularian families terminal investment strategies such as genital mutilation, male sacrifice behavior or monogamy can be associated with a termination of spermiogenesis resulting in a permanent depletion of sperm within the primary reproductive system (Michalik et al., 2010; Michalik and Rittschof, 2011; Schneider and Michalik, 2011).

Evolution of sperm transfer forms in Dysderoidea. The occurrence of two types of STF within one family (Orsolobidae) provides new insights in the evolution of STF in spiders in general and Dysderoidea (Segestriidae, Dysderidae, Orsolobidae, and Oonopidae) especially.

Based on the present study and information available in the literature (Table 3), synspermia are known from Caponiidae and most Dysderoidea (Segestriidae, Dysderidae, and Orsolobidae). Moreover, this sperm conjugation is also known from

Fig. 7. Characteristics of mature spermatozoa and 3D-reconstruction of STF of *Tasmanoonops* sp. 1. **A**: Synspermia contain two sperm that are arranged opposed to each other. The overall shape of sperm conjugates is very similar to those of *T. alipes*, which is continued for sperm characters of both species. **B**: In contrast to *T. alipes*, synspermia of *Tasmanoonops* sp. 1 are not covered with a secretion sheath. The electron dense vesicular area is provided with small, electron lucent spherules (arrows) that are in close association to the membrane that surrounds the syncytium. **C**: The base of the distal centriole is associated with little electron dense material (arrows). **D**: As in all other investigated orsolobids, a distinct amount of glycogen (asterisk) is present around the axonemal base and alongside proximal parts of the axoneme. AF, acrosomal filament; AV, acrosomal vacuole; Ax, axoneme; Mi, mitochondria; NC, nuclear canal; peN, postcentriolar elongation of nucleus; prcN, precentriolar portion of nucleus; SyM, membrane of syncytium; VA, vesicular area.

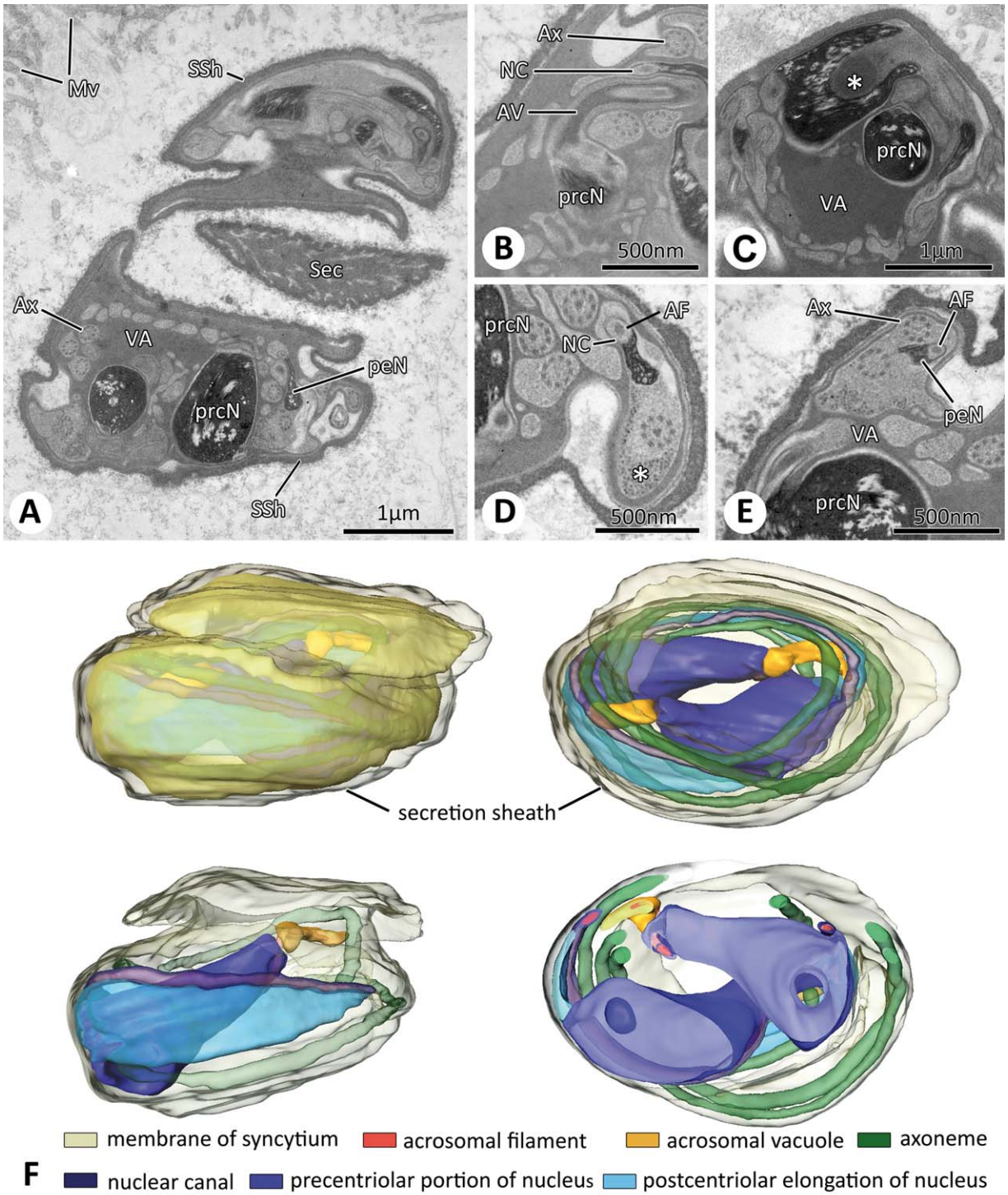

Fig. 8. Characteristics of mature spermatozoa and 3D-reconstruction of STF of *Tasmanoonops* sp. 2. **A**: Besides synspermia, large secretions are present in the lumen of the distal part of the deferent ducts. **B**: The AV is provided with a narrow subacrosomal space in which the AF extends toward the nucleus. **C**: The implantation fossa is completely filled with an electron dense centriolar adjunct (asterisk). A distinct vesicular area encloses the sperm cell components secondarily. **D**: Cross-sections reveal some parts of the membrane surrounding the syncytium distorted from the surrounding secretions sheath, which might result from fixation artifacts. Glycogen is present around the axoneme (asterisk). **E:** Although the AF nearly extends until the end of the NC (D), the central tubuli of the axoneme are very short and not visible in large parts. **F**: In contrast to the cup-like shape of sperm conjugates of *T. alipe*s, synspermia of *Tasmanoonops* sp. 2 appear twisted. As in *T. alipes*, the spermatozoa are arranged opposed to each other while their AVs are bending round parts of the axonemes. AF, acrosomal filament; AV, acrosomal vacuole; Ax, axoneme; Mv, microvilli; NC, nuclear canal; peN, postcentriolar elongation of nucleus; prcN, precentriolar portion of nucleus; Sec, secretions; SSh, secretion sheath; VA, vesicular area.

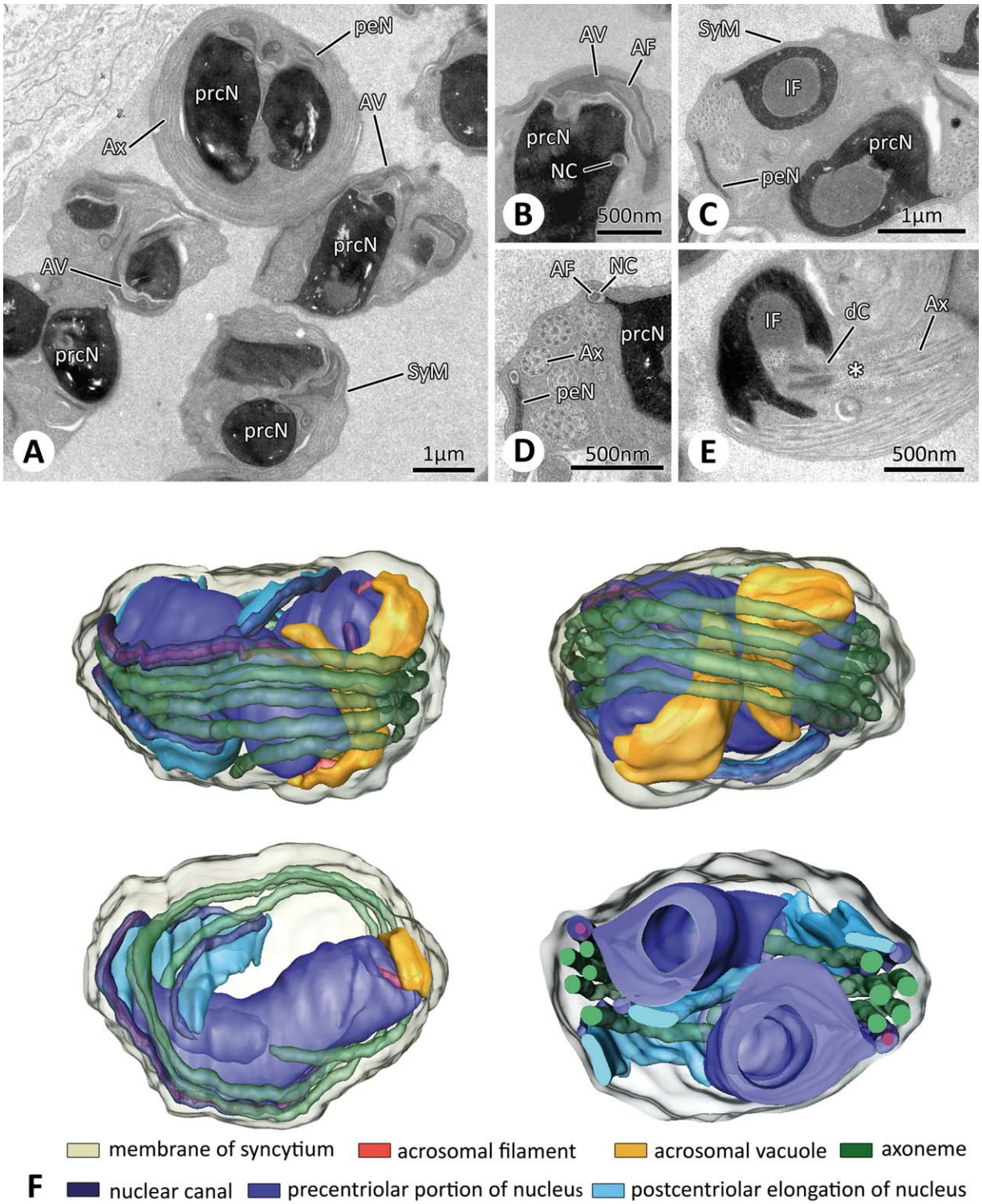

Fig. 9. Characteristics of mature spermatozoa and 3D-reconstruction of *Hickmanolobus mollipes*. **A**: Within the lumen of the distal deferent ducts numerous synspermia are visible. In contrast to most other investigated Orsolobidae, synspermia of *H. mollipes* are not surrounded by a secretion sheath. **B**: The long AV has a narrow subacrosomal space and is separated from the nucleus by a distinct electron dense border. **C**: Two sperm fuse to form the sperm conjugate, cell components of both sperm are surrounded secondarily by a vesicular area. **D**: The NC is situated on a distinct crest before continued in the periphery of the postcentriolar elongation. **E**: A centriolar adjunct, filling the implantation fossa covers both centrioles before glycogen accompanies the base of the axoneme (asterisk). **F**: Both sperm are arranged in the same direction, indicated by the same position of the AVs. AF, acrosomal filament; AV, acrosomal vacuole; Ax, axoneme, dC, distal centriole; IF, implantation fossa; NC, nuclear canal; peN, postcentriolar elongation of nucleus; prcN, precentriolar portion of nucleus; SyM, membrane of syncytium.

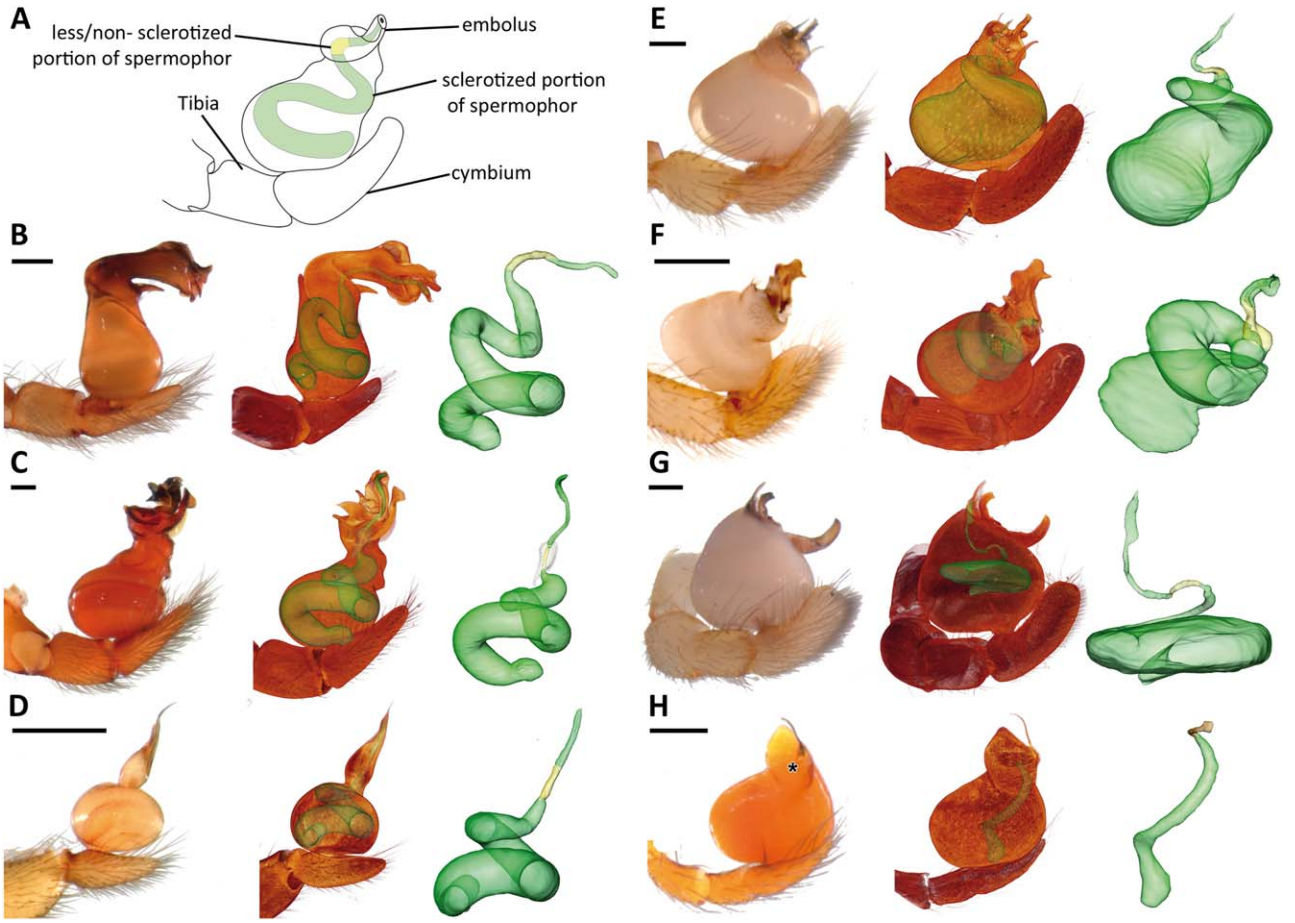

Fig. 10. 3D-reconstructions of the male palpal organ and spermophor. **A**: Schematic drawing of the spermophor in the male palpal organ. Strongly sclerotized parts of the sperm duct are shown in green, a "softer, membranous-like" part in yellow. **B**: *Orsolobus pucara*. **C**: *Osornolobus* sp. 1. **D**: *Osornolobus* sp. 2. **E**: *Tasmanoonops alipes*. **F**: *Tasmanoonops* sp. 1. **G**: *Tasmanoonops* sp. 2. **H**: *Hickmanolobus mollipes*.

Sicariidae (Costa-Ayub and Faraco, 2007) and Scytodidae (Alberti and Weinmann, 1985) suggesting synspermia as a synapomorphy for ecribellate Haplogynae. Our data also support an independent evolution of cleistospermia, which was already suggested by Alberti (1990) and Alberti and Coyle (1991). Because the transformation from sperm conjugates toward cleistospermia occurs even on the genus-level in orsolobids, the evolution toward individual transferred spermatozoa can be expected in many more spider taxa.

In Dysderoidea, synspermia either evolved from coenospermia that are described for Filistatidae (Alberti and Weinmann, 1985; Michalik et al., 2003) or represent fused cleistospermia. Both evolutionary scenarios of STF are already hypothesised by Lipke and Michalik (2012) based on suggestions of Alberti (1990) and Alberti and Coyle (1991).

Secretion Sheath. In general, spider sperm are transferred immobile because the main cell components are coiled within the cytoplasm and the sperm is surrounded by a secretion sheath (Alberti, 1990, 2000; Michalik and Lipke, 2013), i.e., they are encapsulated, as reviewed by Vöcking et al. (2013). The secretion sheath, whose thickness can vary remarkably, is either synthesized in the testes or deferent ducts and can be single or multilayered (Alberti, 1990; Michalik et al., 2013; Michalik and Lipke, 2013). Our data show a high variation concerning the sheath thickness in Orsolobidae. Sperm conjugates of *O. pucara* possess the thickest secretion sheath (~450 nm), whereas a thin secretion sheath surrounds the sperm conjugates of *Osornolobus* sp. 1, *Tasmanoonops alipes*, and *Tasmanoonops* sp. 2. We could not detect a secretion sheath surrounding synspermia of *H. mollipes and Tasmanoonops* sp. 1 (Figs. 7 and 9). Except for the peculiar sperm of *Phoroncid*a sp. (Theridiidae), which is neither coiled nor encapsulated (Lopez and Boissin, 1975; Alberti, 1990), there is only one description of sperm conjugates of a Caponiidae, *C. alegre*, (Lipke and Michalik, 2012) available, where a secretions sheath was not observed (Table 3).

Lipke and Michalik (2012) suggested that a secretion sheath might not be applied before sperm induction or even be generated in the palpal bulb.

TABLE 2. Selected sperm characters of Orsolobidae compared to sperm traits of the remaining Dysderoidea (Segestriidae, Dysderidae, and Oonopide) and Caponiidae, reviewed from the literature

	Caponiidae	Segestriidae	Dysderidae	Orsolobidae							Oonopidae
	Caponina alegre	*Segestria senoculata*	Several species of genus *Dysdera, Harpactea; Dasumia taeniifera*	*Orsolobus pucara*	*Osornolobus* sp. 1	*Osornolobus* sp. 2	*Tasmanoonops alipes*	*Tasmanoonops* sp. 1	*Tasmanoonops* sp. 2	*Hickmanolobus mollipes*	*Oonops domesticus*
	Lipke and Michalik 2012	Alberti and Weinmann 1985	Alberti and Weinmann 1985; Michalik et al. 2004	Present study							Alberti und Weinmann 1985; Burger and Michalik 2010
Genital system											
Testes	Proximally fused	Paired	proximally fused	Paired	Paired	Paired	Paired	Paired	Paired	Paired	Completely fused
Shape of testes	U-shaped	Elongated	U-shaped	Elongated	Elongated	Elongated	Elongated	Elongated	Elongated	Oval	Spherical
Selected characters											
Vesicular area	Present	Absent	Present	Absent	Absent	Absent	Present	Present	Present	Present	Present
AV	Cylindrical	Conical	Cylindrical	Cylindrical	Cylindrical	Conical	Conical	Conical	Conical	Conical	Cylindrical
Length of AV (prcN:AV)	4.8 μm (~15:1)	No measurements available	(2:1)	2.9 μm (~3:1)	2.6 μm (~4:1)	2.7 μm (~2:1)	2.4 μm (~2:1)	1.6 μm (~2:1)	1.7 μm (~2:1)	2.6 μm (~2:1)	No measurements available
AF	Terminated before end of NC	Terminated before end of NC	Terminated before end of NC	Extends to the end of NC	Extends to the end of NC	Extends to the end of NC	Extends to the end of NC	Extends to the end of NC	Extends to the end of NC	Extends to the end of NC	Terminated before end of NC
IF (prcN:IF)	short (~15:1)	Short	medium (~ 5:1)	(~5:1)	(~8:1)	(~8:1)	(~5:1)	(~4:1)	(~8:1)	(~3:1]	large (~ 3:1, widened)
Content of IF (except centrioles)	None	None	ca	ca	ca	ca	ca	ca	ca	ca	none
Total length of N	76.2 μm	No measurements available	No measurements available	13.3 μm	15.4 μm	13 μm	8.4 μm	6.5 μm	8.6 μm	10.5 μm	No measurements available
Length of prcN	73.7 μm	No measurements available	No measurements available	7.2 μm	9.8 μm	6.5 μm	5.2 μm	2.9 μm	4.0 μm	4.7 μm	No measurements available
Length of peN	2.5 μm	No measurements available	No measurements available	6.1 μm	5.6 μm	6.5 μm	3.2 μm	3.6 μm	4.6 μm	5.8 μm	No measurements available
Relation prcN:peN	(~30:1)	No measurements available	(~ 1:2)	(~1:1)	(~2:1)	(~1:1)	(~1,5:1)	(~1:1)	(~1:1)	(~1:1)	No measurements available
Position of NC	Intermediate (first central than stalked peripherally)	Peripheral	Peripheral, on narrow ridge posteriorly	Peripheral, on narrow ridge posteriorly	Peripheral, on narrow ridge posteriorly	Peripheral, small ridge posteriorly	Peripheral	Peripheral	Peripheral	Peripheral, small ridge posteriorly	Peripheral

Table 2. (continued).

	Caponiidae	Segestriidae	Dysderidae	Orsolobidae							Oonopidae
	Caponina alegre	*Segestria senoculata*	Several species of genus *Dysdera, Harpactea; Dasumia taeniifera*	*Orsolobus pucara*	*Osornolobus* sp. 1	*Osornolobus* sp. 2	*Tasmanoonops alipes*	*Tasmanoonops* sp. 1	*Tasmanoonops* sp. 2	*Hickmanolobus mollipes*	*Oonops domesticus*
	Lipke and Michalik 2012	Alberti and Weinmann 1985	Alberti and Weinmann 1985; Michalik et al. 2004	Present study							Alberti und Weinmann 1985; Burger and Michalik 2010
Glycogen around axonemal base	Present	Present	Present (+ alongside peN)	Present	Present	Present	Present	Present	Present	Present	Present
Length of Ax	51.9 μm	No measurements available	No measurements available	No measurements available	51.9 μm	34.6 μm	25.1 μm	19.5 μm	20.9 μm	28.4 μm	No measurements available
Relation Ax : N	Ax < N	Ax > N	Ax > N	No measurements available	Ax > N	Ax > N	Ax > N	Ax > N	Ax > N	Ax > N	Ax > N

Abbreviation: AF, acrosomal filament; AV acrosomal vacuole; Ax, axoneme; ca, centriolar adjunct; IF, implantation fossa; N, nucleus (prcN + peN); NC, nuclear canal; peN, post-centriolar elongation of nucleus; prcN, precentriolar region of nucleus.

TABLE 3. Sperm transfer forms within Dysderoidea as constituted from the present study and information reviewed in the literature

	Caponiidae	Segestriidae	Dysderidae		Orsolobidae							Oonopidae
Reference	Lipke and Michalik, 2012	Alberti and Weinmann, 1985	Michalik et al. 2004; Alberti and Weinmann, 1985	Michalik et al., 2004	Present study							Alberti and Weinmann, 1985
Genus	*Caponina*	*Segestria*	*Dysdera*	*Harpactea*	*Orsolobus*	*Osornolobus*		*Tasmanoonops*		*Hickmanolobus*		*Oonops*
Species	*Caponina alegre*	*Segestria senoculata*	*several*	*several*	*Orsolobus pucara*	*Osornolobus* sp. 1	*Osornolobus* sp. 2	*Tasmanoonops alipes*	*Tasmanoonops* sp.1	*Tasmanoonops* sp.2	*Hickmanolobus mollipes*	*Oonops domesticus*
Sperm transfer form	Synspermia	Synspermia	Synspermia	Synspermia	Synspermia	Synspermia	Cleistospermia	Synspermia	Synspermia	Synspermia	Synspermia	Cleistospermia
# of sperm	4	4	4	2	16/32	4	1	2	2	2	2	1
Secretion sheath	Absent	Present	Present	Present	Present	Present	Present	Present	Absent	Present	Absent	Present

species	dimensions of sperm transfer forms	thinnest portion of spermophor
Orsolobus pucara (16 sperm)	8.5 x 8.5 x 8.5 µm	16.5 x 9.0 µm
Orsolobus pucara (32 sperm)	11.0 x 11.0 x 11.0 µm	16.5 x 9.0 µm
Osornolobus sp. 1	5.5 x 5.5 x 5.0 µm	16.5 x 11.0 µm
Osornolobus sp. 2	4.0 x 4.5 x 4.0 µm	8.5 x 8.5 µm
Tasmanoonops alipes	4.0 x 4.0 x 4.0 µm	10.0 x 7.0 µm
Tasmanoonops sp. 1	3.5 x 4.0 x 4.0 µm	20.5 x 15.5 µm
Tasmanoonops sp. 2	5.5 x 4.0 x 5.5 µm	6.5 x 6.5 µm
Hickmanolobus mollipes	3.5 x 4.0 x 4.0 µm	9.5 x 6.5 µm

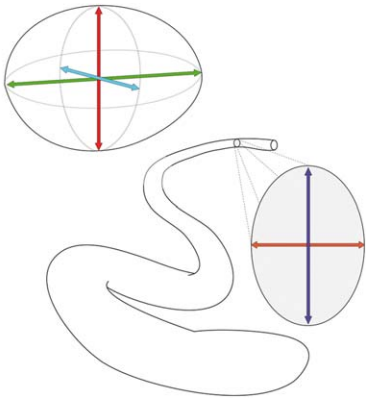

Fig. 11. Dimensions of STF and the thinnest portion of the spermophor (DoS) inside the embolus of all investigated Orsolobidae. The dimensions of STF were measured based on the largest extension of individual STF in each plane (XY/XZ/YZ) of the corresponding image stack that was used for 3D-reconstruction. Dimensions of the spermophor are based on cross-sections of its thinnest portion.

However, the absence of a secretion sheath in sperm conjugates of Orsolobidae indicates that this condition might be common in spiders.

We suggest using the term *unsheathed* as prefix for transfer forms without secretion sheath. So far, all known STF lacking a secretion sheath are primary sperm conjugates, which might possibly suggest a correlation between this specialized transfer form and the functional significance of a secretion sheath. However, the purpose of the secretion sheath is still unknown, although a putative protective function during sperm transfer into the female genitalia (Bertkau, 1877; Alberti, 1990), and storage in female spermathecae was suggested (Michalik et al., 2013). In the wolf spider *Schizocosa malitiosa*, for example, female store sperm for several months (Costa and Capocasale, 1985; Costa, 1991) before egg sacs are laid, whereas the transferred sperm are provided with a thick secretion sheath of approximately 400 nm (Michalik et al., 2013). Thus, there might be a correlation of sperm residency time in female spermathecae and thickness of the secretion sheath. Consequently, unsheathed primary sperm conjugates might indicate a rather short residency time in female spermathecea.

However, transferring unsheathed sperm conjugates might refer to a highly specialized male mating strategy. In spiders, female sperm storage sites are associated with accessory glandular units, whose secretory products are supposed to trigger processes such as decapsulation and sperm activation and might enable the female to selectively activate sperm (Uhl, 1993, 1994, 2000; Herberstein et al., 2011; Vöcking et al., 2013). Thus, the absence of a secretion sheath might provide a male strategy in which sperm bypass the initial triggering that is otherwise controlled by female secretory products. However, if the secretion sheath has a protective function during sperm induction and transfer, unsheathed sperm should hypothetically be provided with additional secretions which might act as a protection shield.

Male Copulatory Organs and STF. Male and female reproductive systems, as well as parts of them, often coevolve (Arnqvist and Rowe, 1995; Eberhard, 2004a, 2004b; Hosken and Stockley, 2004; Simmons, 2014). Besides modifications of the male copulatory organ, the organization of the female reproductive tract, especially sperm storage sites, influence the evolution of sperm traits as it is best known for insects (Presgraves et al., 1999; Miller and Pitnick, 2002; Higginson et al., 2012a, 2012b). Moreover, postcopulatory sexual selection is in charge of rapid diversification of reproductive characters (Lüpold et al., 2013; Manier et al., 2013b) and consequently promotes reproductive isolation (Manier et al., 2013a). A positive correlation of sperm size and female sperm storage organs is known for a variety of taxa, as, for example, birds (Briskie and Montgomerie, 1992), and several insect taxa (Dybas and Dybas, 1981; Pitnick et al., 1999; Presgraves et al., 1999; Higginson et al., 2012b). Because variability of sperm size usually reflects sperm length, a positive correlation of sperm length and female sperm storage organs was suggested. However, spider sperm are usually coiled and encapsulated while transferred into the female genital tract, thus sperm size can be treated as equivalent to the size of the STF by means of diameter at first. Moreover, besides morphological features of female genitalia, initially sperm need to pass the embolus of the male copulatory organs, which is inserted into the female while copulation.

A positive correlation of the size of STF and diameter of opening of the embolus was proposed by Alberti and Coyle (1991) and Michalik et al. (2004b). As summarized in Fig. 11, we observed a considerable variation in the thinnest portion of most distal part of the spermophor (DoS) and dimensions of STF within Orsolobidae.

However, not only the size but also the number and arrangement of spermatozoa in one STF varies. For example, *O. pucara* seem to be limited

to pass one sperm conjugate at once, due to the DoS to STF ratio (Fig. 11), but up to 32 individual sperm are transferred in a single conjugate (Table 3). Passing such a large number of sperm at once would imply a hypothetical DoS that is three times larger in, for example, *Osornolobus* sp. 1 that transfer small sperm conjugates, or even 16 times larger in *Osornolob*us sp. 2, which transfers individual cleistospermia. Kuntner et al. (2009) showed that the complexity of male and female genital traits in nephiliid taxa is positively correlated, best explained with coevolving genital traits. This coevolution likely includes the DoS of the male copulatory organ. Consequently, genital traits of both, female and male, might affect the evolution of STF.

ACKNOWLEDGMENTS

The authors thank K. Huckstorf (University of Rostock), M.A. Izquierdo (Museo Argentino de Ciencias Naturales, Buenos Aires), and C.S. Wirkner (University of Rostock) for collecting and C. Grismado (Museo Argentino de Ciencias Naturales, Buenos Aires) for determining species. We wish to thank M. Frank, G. Fulda, and W. Labs (all Center for Electron Microscopy, University of Rostock) for their kind admission to use the Carl Zeiss EM 902 transmission electron microscope and helpful support. Furthermore we thank G. Alberti (University of Greifswald) for helpful discussions, as well as G. Uhl (University of Greifswald) for her support, two anonymous reviewers, and the editor for their helpful comments on the manuscript.

LITERATURE CITED

Afzelius BA, Dallai R. 1987. Conjugated spermatozoa. In: Mohri H, editor. New Horizons in Sperm Cell Research. Tokyo, New York, London, Paris, Montreaux, Tokyo: Japan Scientific Societies Press Gordon and Breach Scientific Publishers. pp 349–355.

Alberti G. 1990. Comparative spermatology of Araneae. Acta Zool Fenn 190:17–34.

Alberti G. 2000. Chelicerata. In: Adiyodi KG, Adiyodi RG, editors. Reproductive Biology of Invertebrates. Queensland: Oxford & IBH Publishing Co. pp 311–388.

Alberti G, Coyle FA. 1991. Ultrastructure of the primary male genital system, spermatozoa, and spermiogenesis of *Hypochilus pococki* (Araneae, Hypochilidae). J Arachnol 19:136–149.

Alberti G, Weinmann C. 1985. Fine structure of spermatozoa of some labidognath spiders (Filistidae, Segestriidae, Dysderidae, Oonopidae, Scytodidae, Pholcidae; Araneae; Arachnida) with remarks on spermiogenesis. J Morphol 185:1–35.

Alberti G, Afzelius BA, Lucas SM. 1986. Ultrastructure of spermatozoa and spermatogenesis in bird spiders (Theraphosidae, Mygalomorphae, Araneae). J Submicrosc Cytol 18:739–753.

Arnaud L, Haubruge E, Gage MJG. 2001. Sperm size and number variation in the red flour beetle. Zool J Linn Soc 133:369–375.

Arnqvist G, Rowe L. 1995. Sexual conflict and arms races between the sexes: A morphological adaptation for control of mating in a female insect. Proc R Soc B: Biol Sci 261:123–127.

Baehr B, Smith HM. 2008. Three new species of the Australian orsolobid genus *Hickmanolobus* (Araneae: Orsolobidae). Rec West Aus Mus 24:325–336.

Baehr B, Raven RJ, Hebron W. 2011. Orsolobidae of the IBISCA-Queensland project at Lamington national park. Memoires of the Queensland Museum. Nature 55:439–449.

Bertkau P. 1877. Über die Übertragungsorgane und die Spermatozoen der Spinnen. Verh Nat Ver Preuss Rheinlande 34:28–32.

Briskie JV, Montgomerie R. 1992. Sperm size and sperm competition in Birds. Proc Roy Soc B: Biol Sci 247:89–95.

Briskie JV, Montgomerie R, Birkhead TR. 1997. The evolution of sperm size in birds. Evolution 51:937–945.

Burger M. 2010. Complex female genitalia indicate sperm dumping in armored goblin spiders (Arachnida, Araneae, Oonopidae). Zoology (Jena) 113:19–32.

Burger M. 2011. Functional morphology of female goblin spider genitalia (Arachnida: Araneae: Oonopidae) with notes on fertilization in spiders. Zool Anz: J Comp Zool 250:123–133.

Burger M, Graber W, Michalik P, Kropf C. 2006. *Silhouettella loricatula* (Arachnida, Araneae, Oonopidae): A Haplogyne spider with complex female genitalia. J Morphol 267:663–677.

Burger M, Izquierdo MA, Carrera P. 2010. Female genital morphology and mating behavior of *Orchestina* (Arachnida:Araneae:Oonopidae). Zoology 113:100–109.

Burger M, Michalik P. 2010. The Male Genital System of Goblin Spiders: Evidence for the Monophyly of Oonopidae (Arachnida: Araneae). Am Mus Novit 3675:1–13.

Costa-Ayub CLS, Faraco CD. 2007. Ultrastructural aspects of spermiogenesis and synspermia in the brown spider Loxosceles intermedia (Araneae: Sicariidae). Arthropod Struct Dev 36:41–51.

Costa FG. 1991. Fenología de *Lycosa malitiosa* Tullgren (Araneae, Lycosidae) como componente del criptozoos en Marindia, localidad costera del sur de Uruguay. Bol Soc Zool Uruguay 6:8–21.

Costa FG, Capocasale RM. 1985. La producción de ootecas de *Lycosa malitiosa* Tullgren (Araneae, Lycosidae). III. Distribución temporal de las oviposiciones. Aracnología 5:1–14.

Dallai R, Afzelius BA, Witalinski W. 1995. The axoneme of the spider spermatozoon. Boll Zool 62:335–338.

Dybas LK, Dybas HS. 1981. Coadaptation and taxonomic differentiation of sperm and spermathecae in featherwing beetles. Evolution 35:168–174.

Eberhard WG. 2004a. Male-female conflict and genitalia: Failure to confirm predictions in insects and spiders. Biol Rev 79: 121–186.

Eberhard WG. 2004b. Rapid divergent evolution of sexual morphology: Comparative test of antagonistic coevolution and traditional female choice. Evolution 58:1947–1970.

Forster RR, Platnick NI. 1985. A review of the austral spider family Orsolobidae (Arachnida, Araneae) with notes on the superfamily Dysderoidea. Bull Am Nat Hist 181:1–230.

Griswold CE, Ramírez MJ, Coddington JA, Platnick NI. 2005. Atlas of phylogenetic data for entelegyne spiders (Araneae: Araneomorphae: Entelegynae) with comments on their phylogeny. Proc Calif Acad Sci 56 (Suppl. II):1–325.

Herberstein ME, Schneider JM, Uhl G, Michalik P. 2011. Sperm dynamics in spiders. Behav Ecol 22:692–695.

Hickman VV. 1932. Studies in Tasmananian spiders Part 5. Papers Proc R Soc Tasmania 1931:20–31.

Hickman VV. 1979. Some Tasmanian spiders of the families Oonopidae, Anapidae and Mysmenidae. Papers Proc R Soc Tasmania 113:53–79.

Higginson DM, Pitnick S. 2011. Evolution of intra-ejaculate sperm interactions: Do sperm cooperate? Biol Rev Camb Philos Soc 86:249–270.

Higginson DM, Miller KB, Segraves KA, Pitnick S. 2012a. Convergence, recurrence and diversification of complex sperm traits in diving beetles (Dytiscidae). Evolution 66:1650–1661.

Higginson DM, Miller KB, Segraves KA, Pitnick S. 2012b. Female reproductive tract form drives the evolution of complex sperm morphology. Proc Natl Acad Sci USA 109:4538–4543.

Hosken DJ. 2003. Sperm biology: Size indeed matters. Curr Biol 13:R355–R356.
Hosken D, Stockley P. 2004. Sexual selection and genital evolution. Trends Ecol Evol 19:87–93.
Huber BA. 2005. High species diversity, male-female coevolution, and metaphyly in Southeast Asian pholcid spiders: The case of *Belisana* Thorell 1898 (Araneae, Pholcidae). Zoologica 155:1–126.
Huber BA. 2006. Cryptic female exaggeration: The asymmetric female internal genitalia of Kaliana yuruani (Araneae : Phoicidae). J Morphol 267:705–712.
Huber BA, González AP. 2001. Female genital dimorphism in a spider (Araneae: Pholcidae). J Zool 255:301–304.
Huber BA, Brescovit AD, Rheims CA. 2005. Exaggerated female genitalia in two new spider species (Araneae: Pholcidae), with comments on genital evolution by female choice versus antagonistic coevolution. Insect Syst Evol 36:285–292.
Jamieson BGM. 1987. The ultrastructure and phylogeny of insect spermatozoa. The Edinburgh Building, Cambridge: Cambridge University Press. 320 p.
Kuntner M, Coddington JA, Schneider JM. 2009. Intersexual arms race? Genital coevolution in nephilid spiders (Araneae, Nephilidae). Evolution 63:1451–1463.
LaMunyon CW, Ward S. 2002. Evolution of larger sperm in response to experimentally increased sperm competition in Caenorhabditis elegans. Proc Biol Sci 269:1125–1128.
Lipke E, Michalik P. 2012. Formation of primary sperm conjugates in a haplogyne spider (Caponiidae, Araneae) with remarks on the evolution of sperm conjugation in spiders. Arthropod Struct Dev 41:561–573.
Lopez A, Boissin L. 1975. Observation de spermatozoides non enkystés chez une araignée du genre *Phoroncidia* (Araneae, Theridiidae). Bull Soc Zool France 100:583–587.
Lüpold S, Pitnick S, Berben KS, Blengini CS, Belote JM, Manier MK. 2013. Female mediation of competitive fertilization success in *Drosophila melanogaster*. Proc Natl Acad Sci USA 110:10693–10698.
Manier MK, Belote JM, Berben KS, Lüpold S, Ala-Honkola O, Collins WF, Pitnick S. 2013a. Rapid diversification of sperm precedence traits and processes among three sibling Drosophila species. Evolution 67:2348–2362.
Manier MK, Lüpold S, Belote JM, Starmer WT, Berben KS, Ala-Honkola O, Collins WF, Pitnick S. 2013b. Postcopulatory sexual selection generates speciation phenotypes in Drosophila. Curr Biol 23:1853–1862.
Michalik P. 2009. The male genital system of spiders (Arachnida, Araneae) with notes on the fine structure of seminal secretions. Contrib Nat Hist 12:959–972.
Michalik P, Alberti G. 2005. On the occurence of the 9+0 axonemal pattern in the spermatozoa of sheetweb spiders (Linyphiidae, Araneae). J Arachnol 33(2):569–572.
Michalik P, Hormiga G. 2010. Ultrastructure of the spermatozoa in the Spider Genus Pimoa: New Evidence for the Monophyly of Pimoidae plus Linyphiidae (Arachnida: Araneae). Am Mus Novit 3682:1–17.
Michalik P, Rittschof CC. 2011. A Comparative Analysis of the Morphology and Evolution of Permanent Sperm Depletion in Spiders. PLoS ONE 6:1.
Michalik P, Lipke E. 2013. Male reproductive system of spiders. In: Nentwig W, editor. Spider Ecophysiology. Heidelberg: Springer.
Michalik P, Ramirez MJ. 2013. First description of the male of *Thaida chepu* Platnick, 1987 (Araneae, Austrochilidae) with micro-computed tomography of the palpal organ. ZooKeys 352:117–125.
Michalik P, Gray MR, Alberti G. 2003. Ultrastructural observations of spermatozoa and spermiogenesis in *Wandella orana* Gray, 1994 (Araneae: Filistatidae) with notes on their phylogenetic implications. Tissue Cell 35:325–337.
Michalik P, Aisenberg A, Postiglioni R, Lipke E. 2013. Spermatozoa and spermiogenesis of the wolf spider *Schizocosa malitiosa* (Lycosidae, Araneae) and its functional and phylogenetic implications. Zoomorphology 132:11–21.
Michalik P, Dallai R, Giusti F, Alberti G. 2004a. The ultrastructure of the peculiar synspermia of some Dysderidae (Araneae, Arachnida). Tissue Cell 36:447–460.
Michalik P, Haupt J, Alberti G. 2004b. On the occurence of coenospermia in mesothelid spiders (Araneae: Heptathelidae). Arthropod Struct Dev 33:173–181.
Michalik P, Knoflach B, Thaler K, Alberti G. 2010. Live for the moment-Adaptations in the male genital system of a sexually cannibalistic spider (Theridiidae, Araneae). Tissue Cell 42: 32–36.
Michalik P, Ramirez M, Wirkner CS, Lipke E. 2014. Morphological evidence for sperm limitation in the enigmatic Tasmanian cave spider *Hickmania troglodytes* (Austrochilidae, Araneae). Invert Biol. DOI: 10.1111/ivb.12046.
Miller GT, Pitnick S. 2002. Sperm-female coevolution in Drosophila. Science 298:1230–1233.
Pitnick S, Markow T, Spicer GS. 1999. Evolution of multiple kinds of female sperm-storage organs in *Drosophila*. Evolution 53:1804–1822.
Pitnick S, Hosken D, Birkhead TR. 2009. Sperm morphological diversity. In: Birkhead TR, Hosken D, Pitnick S, editors. Sperm Biology—An Evolutionary Perspective. Amsterdam: Academic Press. pp 69–149.
Platnick N, Coddington JA, Forster RR, Griswold CE. 1991. Spinneret morphology and the phylogeny of haplogyne spiders (Araneae, Araneomorphae). Am Mus Novit 3016:1–73.
Platnick NI, Abrahim N, Alvarez-Padilla F, Andriamalala D, Baehr BC, Baert L, Bonaldo AB, Brescovit AD, Chousou-Polydouri N, Duperre N, Eichenberger B, Fannes W, Gaublomme E, Gillespie RG, Grismado CJ, Griswold CE, Harvey MS, Henrard A, Hormiga G, Izquierdo MA, Jocque R, Kranz-Baltensperger Y, Kropf C, Ott R, Ramirez MJ, Raven RJ, Rheims CA, Ruiz GRS, Santos AJ, Saucedo A, Sierwald P, Szuts T, Ubick D, Wang XP. 2012. Tarsal Organ Morphology and the Phylogeny of Goblin Spiders (Araneae, Oonopidae), With Notes on Basal Genera. Am Mus Novit 3736:1–52.
Presgraves DC, Baker RH, Wilkinson GS. 1999. Coevolution of sperm and female reproductive tract morphology in stalked-eyed flies. Proc R Soc B: Biol Sci 266:10411047.
Ramirez MJ. 2000. Respiratory system morphology and the phylogeny of Haplogyne spiders (Araenae, Araneomorphae). J Arachnol 28:149–157.
Reynolds ES. 1963. The use of lead citrate at high pH as electron-opaque stain in electron microscopy. J Cell Biol 17: 208–212.
Richardson HH, Jarett L, Finke EH. 1960. Embedding in Epoxy Resins for ultrathin sectioning in electron microscopy. Stain Technol 35:313–323.
Saalfeld S, Fetter R, Cardona A, Tomancak P. 2012. Elastic volume reconstruction from series of ultra-thin microscopy sections. Nat Methods 9:717–720.
Schneider JM, Michalik P. 2011. One-shot genitalia are not an evolutionary dead end—Regained male polygamy in a sperm limited spider species. BMC Evol Biol 11:197.
Simmons LW. 2014. Sexual selection and genital evolution. Austral Entomol 53:1–17.
Spurr AR. 1969. A low-viscosity epoxy resin embedding medium for electron microscopy. J Ultrastruct Res 26:31–43.
Uhl G. 1993. Mating behaviour and female sperm storage in *Pholcus phalangioides* (Fuesslin) (Araneae). Mem Queensl Mus 33:667–674.
Uhl G. 1994. Ultrastructure of the accessory glands in female genitalia of *Pholcus phalangioides* (Fuesslin, 1771) (Pholcidae; Araneae). Acta Zool: Stockholm 75:13–25.
Uhl G. 2000. Female genital morphology and sperm priority patterns in spiders (Araneae). In: Toft S, Scharff N, editors. European Arachnology 2000. Aarhus: Aarhus University Press. pp 145–156.
Vöcking O, Uhl G, Michalik P. 2013. Sperm Dynamics in Spiders (Araneae): Ultrastructural Analysis of the Sperm Activation Process in the Garden Spider *Argiope bruennichi* (Scopoli, 1772). PLoS ONE 8:e72660.